Figure 2.   Relative expression of GATA-3 mRNA across the menstrual cycle. Data generation, representation, and analysis are identical to that in Figure 1. Pro indicates proliferative; ES. early secretory; MS, midsecretory; LS, late secretory.
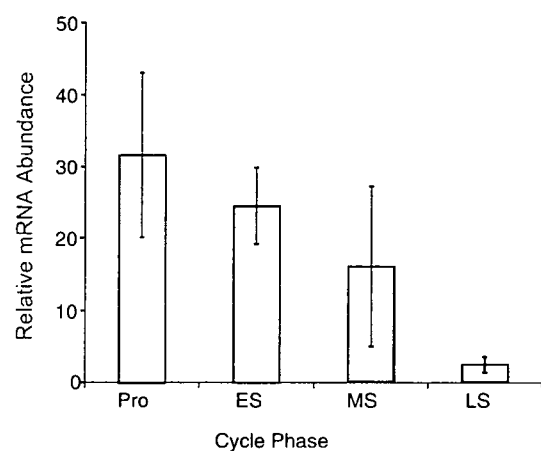

Figure 3.   Relative expression of progesterone receptor mRNA across the menstrual cycle. Data representation and analysis are identical to that in Figure 1. Pro indicates proliferative; ES, early secretory; MS, midsecretory; LS, late secretory.

Figure 4.   Immunohistochemistry. Proliferative (Pro), cycle day 5: early secretory (ES), luteinizing hormone (LH) day 1; midsecretory (MS), LH day 8: late secretory (LS), LH day 12. Magnification 20x.

cycle. Several samples from all phases of the menstrual cycle are represented in Figure 4.

In proliferative samples. both T-Bet and GATA-3 proteins were detected and localized primarily to the cytoplasm of epithelial cells. In contrast. PR was detected in the nuclei of both the epithelial and stromal cells of proliferative samples. T-Bet was also found in a small number of strongly staining smaller cells, likely lymphocytes. In samples from the early secretory phase, GATA-3
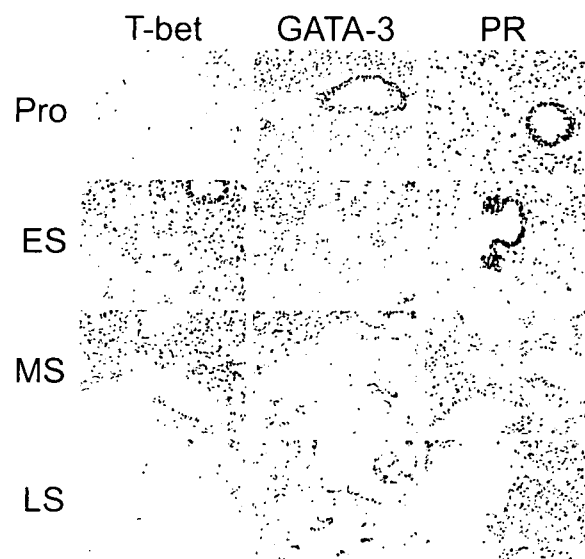
and T-Bet staining was faint and not always detectable, but PR staining was prominent. A few stromal cells were darkly stained for T-Bet. Samples from the midsecretory phase (the implantation window) showed a somewhat reduced intensity of nuclear PR staining and increased cytoplasmic staining for T-Bet and GATA-3 in glandular epithelial cells. In the late secretory phase, PR protein was, as expected, undetectable in the glandular epithelium but clearly detectable in some stromal cells.[19] Late secretory immunostaining for both T-Bet and GATA-3 protein expression was markedly elevated in the cytoplasm of the glandular epithelium. Thus, the intensity of immunohistochemical staining for T-Bet, GATA-3, and PR generally parallels the mRNA changes. Furthermore, the cell types expressing GATA-3 and T-Bet appear to be primarily endometrial epithelium, with a small number of stromal cells (lymphocytes) also positive for T-Bet staining, especially in the proliferative and early secretory phases.

DISCUSSION

Cytokines play key roles in reproductive. immune. and menstrual functions of human endometrium. This study was designed to measure the endometrial expression of 2 transcription factors. T-Bet and GATA-3. known to be

critical regulators of cytokine expression in lymphocytes. We have demonstrated that T-Bet and GATA-3 mRNA and protein are cyclically expressed in human endometrium, predominantly in the epithelial cells. Furthermore, expression of both was shown to be maximal in the late secretory phase, and both proteins were primarily localized to the cytoplasm of endometrial epithelial cells.

The cyclical changes in T-Bet and GATA-3 expression strongly suggest regulation by reproductive steroid hormones. T-Bet promoter activity in an endometrial cell line has been previously shown to be stimulated by treatment with progesterone in vitro, in a time-dependent oscillation.[13] In the same set of experiments, progesterone treatment also stimulated stat5 binding to the T-Bet promoter, possibly via an autocrine feedback loop involving IL-15 activation of stat5. Since endometrial IL-15 expression is increased in the late secretory phase by the action of progesterone on endometrial stromal cells,[21] a paracrine effect of IL-15 may underlie the cyclic expression of T-Bet in the endometrial epithelium. Interestingly, endometrial stromal expression of IL-15 is also induced by co-culture with trophoblast,[22] suggesting a mechanism for possible increased endometrial expression of T-Bet during embryo implantation.

Another potential mechanism of steroid action on T-Bet and GATA-3 expression is via the nuclear factor κB (NF-κB) pathway. Both T-Bet and GATA-3 expression can be stimulated by NF-κB.[23-25] Furthermore, NF-κB activity can be inhibited by both estrogen and progesterone.[26-28] Since estrogen and progesterone and specific subtypes of the estrogen and progesterone receptors are low in the late luteal phase, falling estrogen and progesterone actions may disinhibit NF-κB, leading to increased T-Bet and GATA-3 expression.

In lymphocytes, T-Bet expression and GATA-3 expression are generally mutually exclusive, and the functions of these 2 transcription factors are often antagonistic.[1,18] Despite the antagonism, common factors have been identified that have similar effects on expression of both T-Bet and GATA-3. For instance, in classical immune cells, transforming growth factor–β (TGF-β) has been shown to inhibit both the expression of T-Bet[29,30] and differentiation of T$_H$1-type cells[31,32] and the expression of GATA-3 and differentiation T$_H$2-type cells.[32] Thus, our finding that both GATA-3 and T-Bet are maximally expressed in endometrial epithelia during the late secretory phase, while unexpected, may reflect control through signaling pathways similar to that associated with TGF-β. Interestingly, several TGF-β isoforms are strong

inhibitors of trophoblast outgrowth and proliferation.[33,34] Although the reason for this double-barreled immune response in the late secretory phase involving both T-Bet and GATA-3 remains unclear, both factors can activate the expression of cox-2, IL-8, monocyte chemotactic protein, and IL-2, all of which play functional roles in immune cell migration, inflammation, and tissue breakdown during menstruation.

Another unexpected finding was that both T-Bet and GATA-3 proteins are immunolocalized to the cytoplasm of the glandular epithelium rather than the nucleus, where both transcription factors are thought to function. This cytoplasmic localization suggests either an alternative, nontranscriptional function or a requirement for activation prior to entering the nucleus. Mariani et al,[35] in developing a model of cross-regulation of T-Bet and GATA-3 in T lymphocytes, proposed 3 possible mechanisms of inhibition including sequestration by a binding protein, repression of basal transcription, and repression of autoactivation. One recent study showed that GATA-3 nuclear translocation is dependent on its phosphorylation on serine residues by p38 MAPK[36]; however, the factors determining T-Bet nuclear translocation remain unreported.

T-Bet was also immunolocalized to the nucleus of a small number of stromal cells during the proliferative and early secretory phase. This expression pattern is in contrast to the cytoplasmic expression seen in the glandular cells. These cells are likely lymphocytes or uterine natural killer cells, both of which are known to express T-Bet.[37]

This article localizes T-Bet and GATA-3 to human endometrial epithelial cells histologically and supports previously published endometrial data.[13] Expression of T-Bet and GATA-3 has been characterized in other epithelial tissues, including bronchi and bowel, and alterations in these epithelia-expressed transcription factors have been linked to human disease. GATA-3 is underexpressed while T-Bet is overexpressed in the gut mucosa of celiac disease patients.[38] GATA-3 is upregulated in human bronchial and nasal mucosa in asthmatic subjects compared with controls.[39] However, in each of these cases, the alterations in transcription factor expression patterns that result in functional impairment are presumed or demonstrated to be limited to resident lymphocytes, not epithelial cells. Lymphocyte expression may, in fact, represent only part of the pathogenesis.

Because of the prominent role of cytokines in implantation, menstruation, and endometriosis, it is tempting to speculate that T-Bet and GATA-3 play a role in endometrial

function and dysfunction. However, T-Bet has not been linked to endometrial dysfunction in any article to date, nor has any mention of T-Bet appeared in the various microarray studies examining the physiology and pathophysiology of human endometrium. GATA-3 was shown to be upregulated in eutopic endometrial stromal cells selected by laser capture microdissection from patients with endometriosis.[40] However, GATA-3 microarray data were not confirmed by an alternative method, and no other microarray data have mentioned GATA-3. Thus, it is likely that these cycle-regulated proteins have important effects on endometrial function, but their role remains speculative.

In summary, our data demonstrate GATA-3 and T-Bet expression in human endometrium and suggest hormonal regulation of expression. Furthermore, we demonstrate a somewhat unexpected coexpression of these antagonistic transcription factors and unconventional tissue and subcellular localization. Further studies are required to understand the role of these transcription factors in the physiology and pathophysiology of human endometrium.

REFERENCES

1. Agnello D, Lankford CS, Bream J, et al. Cytokines and transcription factors that regulate T helper cell differentiation: new players and new insights. *J Clin Immunol.* 2003;23(3): 147-161.

2. Zhou M, Ouyang W. The function role of GATA-3 in Th1 and Th2 differentiation. *Immunol Res.* 2003;28(1):25-37.

3. Chaouat G, Zourbas S, Ostojic S, et al. A brief review of recent data on some cytokine expressions at the maternofoetal interface which might challenge the classical Th1/Th2 dichotomy. *J Reprod Immunol.* 2002;53(1-2):241-256.

4. Haynes MK, Smith JB. Can Th1-like immune responses explain the immunopathology of recurrent spontaneous miscarriage? *J Reprod Immunol.* 1997;35(1):65-71.

5. Hill JA III. Choi BC. Immunodystrophism: evidence for a novel alloimmune hypothesis for recurrent pregnancy loss involving Th1-type immunity to trophoblast. *Semin Reprod Med.* 2000;18(4):401-405.

6. Hill JA, Polgar K. Anderson DJ. T-helper 1-type immunity to trophoblast in women with recurrent spontaneous abortion. *JAMA.* 1995;273(24):1933-1936.

7. Piccinni MP. T-cell cytokines in pregnancy. *Am J Reprod Immunol.* 2002;47(5):289-294.

8. Piccinni MP. Beloni L, Livi C, Maggi E. Scarselli G, Romagnani S. Defective production of both leukemia inhibitory factor and type 2 T-helper cytokines by decidual T cells in

unexplained recurrent abortions. *Nat Med.* 1998;4(9): 1020-1024.

9. Piccinni MP, Romagnani S. Regulation of fetal allograft survival by a hormone-controlled Th1- and Th2-type cytokines. *Immunol Res.* 1996;15(2):141-150.

10. Raghupathy R, Makhseed M, Azizieh F, Hassan N, Al-Azemi M, Al-Shamali E. Maternal Th1- and Th2-type reactivity to placental antigens in normal human pregnancy and unexplained recurrent spontaneous abortions. *Cell Immunol.* 1999; 196(2): 122-130.

11. von Wolff M, Thaler CJ, Strowitzki T, Broome J, Stolz W, Tabibzadeh S. Regulated expression of cytokines in human endometrium throughout the menstrual cycle: dysregulation in habitual abortion. *Mol Hum Reprod.* 2000;6(7):627-634.

12. Wegmann TG, Lin H, Guilbert L, Mosmann TR. Bidirectional cytokine interactions in the maternal-fetal relationship: is successful pregnancy a TH2 phenomenon? *Immunol Today.* 1993; 14(7):353-356.

13. Kawana K, Kawana Y, Schust DJ. Female steroid hormones utilize Stat protein-mediated pathways to modulate the expression of T-Bet in epithelial cells: a mechanism for local immune regulation in the human reproductive tract. *Mol Endocrinol.* 2005;19(8):2047-2059.

14. Stewart CL, Kaspar P, Brunet LJ, et al. Blastocyst implantation depends on maternal expression of leukaemia inhibitory factor. *Nature.* 1992;359(6390):76-79.

15. Hambartsoumian E, Taupin JL, Moreau JF, Frydman R, Chaouat G. In-vivo administration of progesterone inhibits the secretion of endometrial leukaemia inhibitory factor in vitro. *Mol Hum Reprod.* 1998;4(11):1039-1044.

16. Bebo BF Jr, Fyfe-Johnson A, Adlard K, Beam AG, Vandenbark AA, Offner H. Low-dose estrogen therapy ameliorates experimental autoimmune encephalomyelitis in two different inbred mouse strains. *J Immunol.* 2001;166(3):2080-2089.

17. Lambert KC, Curran EM, Judy BM, Milligan GN, Lubahn DB, Estes DM. Estrogen receptor alpha (ERalpha) deficiency in macrophages results in increased stimulation of CD4+ T cells while 17beta-estradiol acts through ERalpha to increase IL-4 and GATA-3 expression in CD4+ T cells independent of antigen presentation. *J Immunol.* 2005;175(9):5716-5723.

18. Chen GY, Osada H, Santamaria-Babi LF, Kannagi R. Interaction of GATA-3/T-Bet transcription factors regulates expression of sialyl Lewis X homing receptors on Th1/ Th2 lymphocytes. *Proc Natl Acad Sci U S A.* 2006;103(45): 16894-16899.

19. Young L. Endometriosis in Clinical Practice. Normal Cycling Endometrium. Molecular, Cellular, and Histologic Perspectives. New York. NY: Taylor & Francis; 2004.

20. Noyes RW. Hertig AW. Rock J. Dating the endometrial biopsy. *Fertil Steril* 1950;1(1):3-25.

21. Dunn CL. Critchley HO, Kelly RW. IL-15 regulation in human endometrial stromal cells. *J Clin Endocrinol Metab.* 2002; 87(4):1898-1901

22. Popovici RM, Betzler NK, Krause MS, et al. Gene expression profiling of human endometrial-trophoblast interaction in a coculture model. *Endocrinology*. 2006;147(12):5662-5675.

23. Corn RA, Aronica MA, Zhang F, et al. T cell-intrinsic requirement for NF-kappa B induction in postdifferentiation IFN-gamma production and clonal expansion in a Th1 response. *J Immunol*. 2003;171(4):1816-1824.

24. Das J, Chen CH, Yang L, Cohn L, Ray P, Ray A. A critical role for NF-kappa B in GATA3 expression and TH2 differentiation in allergic airway inflammation. *Nat Immunol*. 2001;2(1):45-50.

25. McCracken SA, Hadfield K, Rahimi Z, Gallery ED, Morris JM. NF-kappaB-regulated suppression of T-Bet in T cells represses Th1 immune responses in pregnancy. *Eur J Immunol*. 2007;37(5):1386-1396.

26. Biswas DK, Singh S, Shi Q, Pardee AB, Iglehart JD. Crossroads of estrogen receptor and NF-kappaB signaling. *Sci STKE*. 2005;2005(288):pe27.

27. Kelly RW, King AE, Critchley HO. Cytokine control in human endometrium. *Reproduction*. 2001;121(1):3-19.

28. King AE, Critchley HO, Kelly RW. The NF-kappaB pathway in human endometrium and first trimester decidua. *Mol Hum Reprod*. 2001;7(2):175-183.

29. Lin JT, Martin SL, Xia L, Gorham JD. TGF-beta 1 uses distinct mechanisms to inhibit IFN-gamma expression in CD4+ T cells at priming and at recall: differential involvement of Stat4 and T-Bet. *J Immunol*. 2005;174(10):5950-5958.

30. Park IK, Letterio JJ, Gorham JD. TGF-beta1 inhibition of IFN-gamma-induced signaling and Th1 gene expression in CD4(+) T cells is Smad3 independent but MAP kinase dependent. *Mol Immunol*. 2007;44(13):3283-3290.

31. Gorelik L, Constant S, Flavell RA. Mechanism of transforming growth factor beta-induced inhibition of T helper type 1 differentiation. *J Exp Med*. 2002;195(11):1499-1505.

32. Gorelik L, Fields PE, Flavell RA. Cutting edge: TGF-beta inhibits Th type 2 development through inhibition of GATA-3 expression. *J Immunol*. 2000;165(9):4773-4777.

33. Caniggia I, Taylor CV, Ritchie JW, Lye SJ, Letarte M. Endoglin regulates trophoblast differentiation along the invasive pathway in human placental villous explants. *Endocrinology*. 1997;138(11):4977-4988.

34. Jones RL, Stoikos C, Findlay JK, Salamonsen LA. TGF-beta superfamily expression and actions in the endometrium and placenta. *Reproduction*. 2006;132(2):217-232.

35. Mariani L, Löhning M, Radbruch A, Höfer T. Transcriptional control networks of cell differentiation: insights from helper T lymphocytes. *Prog Biophys Mol Biol*. 2004;86(1):45-76.

36. Maneechotesuwan K, Xin Y, Ito K, et al. Regulation of Th2 cytokine genes by p38 MAPK-mediated phosphorylation of GATA-3. *J Immunol*. 2007;178(4):2491-2498.

37. Tayade C, Fang Y, Black GP, V A P Jr, Erlebacher A, Croy BA. Differential transcription of Eomes and T-Bet during maturation of mouse uterine natural killer cells. *J Leukoc Biol*. 2005;78(6):1347-1355.

38. Monteleone I, Monteleone G, Del Vecchio Blanco G, et al. Regulation of the T helper cell type 1 transcription factor T-Bet in coeliac disease mucosa. *Gut*. 2004;53(8):1090-1095.

39. Nakamura Y, Hoshino M. TH2 cytokines and associated transcription factors as therapeutic targets in asthma. *Curr Drug Targets Inflamm Allergy*. 2005;4(2):267-270.

40. Matsuzaki S, Canis M, Vaurs-Barrière C, Boespflug-Tanguy O, Dastugue B, Mage G. DNA microarray analysis of gene expression in eutopic endometrium from patients with deep endometriosis using laser capture microdissection. *Fertil Steril*. 2005;84(suppl 2):1180-1190.

Critical role of PA28γ in hepatitis C virus-associated steatogenesis and hepatocarcinogenesis

Kohji Moriishi*, Rika Mochizuki*, Kyoji Moriya[†], Hironobu Miyamoto*, Yoshio Mori*, Takayuki Abe*, Shigeo Murata[‡], Keiji Tanaka[‡], Tatsuo Miyamura[§], Tetsuro Suzuki[§], Kazuhiko Koike[†], and Yoshiharu Matsuura*[¶]

*Department of Molecular Virology, Research Institute for Microbial Diseases, Osaka University, Osaka 565-0871, Japan; [†]Department of Internal Medicine, Graduate School of Medicine, University of Tokyo, Tokyo 113-8655, Japan; [‡]Department of Molecular Oncology, Tokyo Metropolitan Institute of Medical Science, Tokyo 113-8613, Japan; and [§]Department of Virology II, National Institute of Infectious Diseases, Tokyo 162-8640, Japan

Hepatitis C virus (HCV) is a major cause of chronic liver disease that frequently leads to steatosis, cirrhosis, and eventually hepatocellular carcinoma (HCC). HCV core protein is not only a component of viral particles but also a multifunctional protein because liver steatosis and HCC are developed in HCV core gene-transgenic (CoreTg) mice. Proteasome activator PA28γ/REGγ regulates host and viral proteins such as nuclear hormone receptors and HCV core protein. Here we show that a knockout of the PA28γ gene induces the accumulation of HCV core protein in the nucleus of hepatocytes of CoreTg mice and disrupts development of both hepatic steatosis and HCC. Furthermore, the genes related to fatty acid biosynthesis and srebp-1c promoter activity were up-regulated by HCV core protein in the cell line and the mouse liver in a PA28γ-dependent manner. Heterodimer composed of liver X receptor α (LXRα) and retinoid X receptor α (RXRα) is known to up-regulate srebp-1c promoter activity. Our data also show that HCV core protein enhances the binding of LXRα/RXRα to LXR-response element in the presence but not the absence of PA28γ. These findings suggest that PA28γ plays a crucial role in the development of liver pathology induced by HCV infection.

fatty acid | proteasome | sterol regulatory element-binding protein (SREBP) | RXRα | LXRα

H epatitis C virus (HCV) belongs to the Flaviviridae family, and it possesses a positive, single-stranded RNA genome that encodes a single polyprotein composed of ≈3,000 aa. The HCV polyprotein is processed by host and viral proteases, resulting in 10 viral proteins. Viral structural proteins, including the capsid (core) protein and two envelope proteins, are located in the N-terminal one-third of the polyprotein, followed by nonstructural proteins.

HCV infects >170 million individuals worldwide, and then it causes liver disease, including hepatic steatosis, cirrhosis, and eventually hepatocellular carcinoma (HCC) (1). The prevalence of fatty infiltration in the livers of chronic hepatitis C patients has been reported to average ≈50% (2, 3), which is higher than the percentage in patients infected with hepatitis B virus and other liver diseases. However, the precise functions of HCV proteins in the development of fatty liver remain unknown because of the lack of a system sufficient to investigate the pathogenesis of HCV. HCV core protein expression has been shown to induce lipid droplets in cell lines and hepatic steatosis and HCC in transgenic mice (4–6). These reports suggest that HCV core protein plays an important role in the development of various types of liver failure, including steatosis and HCC.

Recent reports suggest that lipid biosynthesis affects HCV replication (7–9). Involvement of a geranylgeranylated host protein, FBL2, in HCV replication through the interaction with NS5A suggests that the cholesterol biosynthesis pathway is also important for HCV replication (9). Increases in saturated and monounsaturated fatty acids enhance HCV RNA replication, whereas increases in polyunsaturated fatty acids suppress it (7). Lipid homeostasis is regulated by a family of sterol regulatory element-binding proteins (SREBPs), which activate the expression of >30 genes involved in

the synthesis and uptake of cholesterol, fatty acids, triglycerides, and phospholipids. Biosynthesis of cholesterol is regulated by SREBP-2, whereas that of fatty acids, triglycerides, and phospholipids is regulated by SREBP-1c (10–14). In chimpanzees, host genes involved in SREBP signaling are induced during the early stages of HCV infection (8). SREBP-1c regulates the transcription of acetyl-CoA carboxylase, fatty acid synthase, and stearoyl-CoA desaturase, leading to the production of saturated and monounsaturated fatty acids and triglycerides (15). SREBP-1c is transcriptionally regulated by liver X receptor (LXR) α and retinoid X receptor (RXR) α, which belong to a family of nuclear hormone receptors (15, 16). Accumulation of cellular fatty acids by HCV core protein is expected to be modulated by the SREBP-1c pathway because RXRα is activated by HCV core protein (17). However, it remains unknown whether HCV core protein regulates the srebp-1c promoter.

We previously reported (18) that HCV core protein specifically binds to the proteasome activator PA28γ/REGγ in the nucleus and is degraded through a PA28γ-dependent pathway. PA28γ is well conserved from invertebrates to vertebrates, and amino acid sequences of human and murine PA28γs are identical (19). The homologous proteins, PA28α and PA28β, form a heteroheptamer in the cytoplasm, and they activate chymotrypsin-like peptidase activity of the 20S proteasome, whereas PA28γ forms a homoheptamer in the nucleus, and it enhances trypsin-like peptidase activity of 20S proteasome (20). Recently, Li and colleagues (21) reported that PA28γ binds to steroid receptor coactivator-3 (SRC-3) and enhances the degradation of SRC-3 in a ubiquitin- and ATP-independent manner. However, the precise physiological functions of PA28γ are largely unknown in vivo. In this work, we examine whether PA28γ is required for liver pathology induced by HCV core protein in vivo.

Results

PA28γ-Knockout HCV Core Gene Transgenic Mice. To determine the role of PA28γ in HCV core-induced steatosis and the development of HCC in vivo, we prepared PA28γ-knockout core gene transgenic mice. The PA28γ-deficient, PA28γ^{−/−} mice were born without
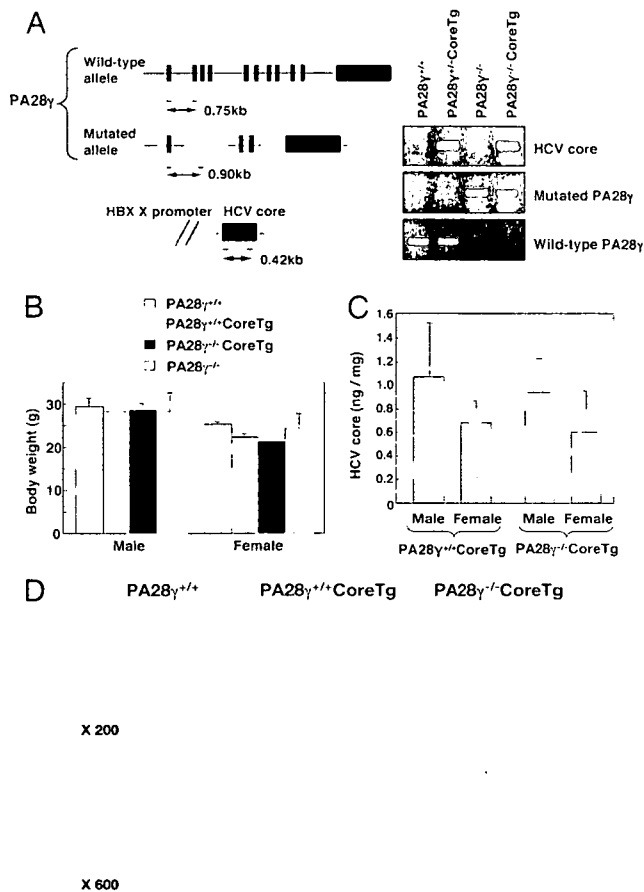
MICROBIOLOGY

Fig. 1. Preparation and characterization of PA28γ-knockout HCV core-transgenic mice. (*A*) The structures of the wild-type and mutated PA28γ genes and the transgene encoding the HCV core protein under the control of the HBV X promoter were investigated. Positions corresponding to the screening primers and sizes of PCR products are shown. PCR products of the HCV core gene as well as wild-type and mutated PA28γ alleles were amplified from the genomic DNAs of PA28γ$^{+/+}$, PA28γ$^{-/+}$CoreTg, PA28γ$^{-/-}$, and PA28γ$^{-/-}$CoreTg mice. (*B*) Body weights of PA28γ$^{+/+}$, PA28γ$^{-/-}$CoreTg, PA28γ$^{-/-}$CoreTg, and PA28γ$^{-/-}$ mice at the age of 6 months. (*C*) HCV core protein levels in the livers of PA28γ$^{+/+}$CoreTg and PA28γ$^{-/-}$CoreTg mice were determined by ELISA (mean ± SD, n = 10). (*D*) Localization of HCV core protein in the liver. Liver sections of PA28γ$^{+/+}$, PA28γ$^{+/+}$CoreTg, and PA28γ$^{-/-}$CoreTg mice at the age of 2 months were stained with anti-HCV core antibody.
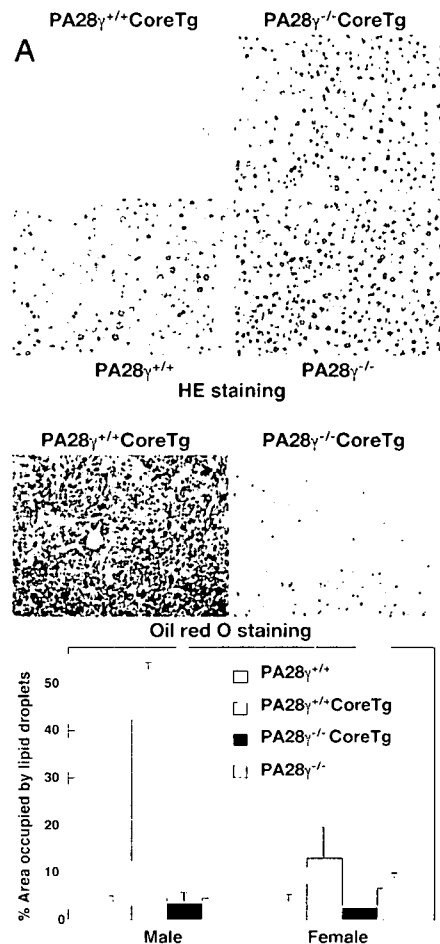

Fig. 2. Accumulation of lipid droplets by expression of HCV core protein. (*A*) Liver sections of the mice at the age of 6 months were stained with hematoxylin/eosin (HE). (*B*) (*Upper*) Liver sections of PA28γ$^{+/+}$CoreTg and PA28γ$^{-/-}$CoreTg mice at the age of 6 months were stained with oil red O. (*Lower*) The area occupied by lipid droplets of PA28γ$^{+/+}$ (white), PA28γ$^{-/+}$CoreTg (gray), PA28γ$^{-/-}$CoreTg (black), and PA28γ$^{-/-}$ (dark gray) mice was calculated by Image-Pro software (MediaCybernetics, Silver Spring, MD) (mean ± SD, n = 10).

appreciable abnormalities in all tissues examined, with the exception of a slight retardation of growth (22). HCV core gene-transgenic (PA28γ$^{+/+}$CoreTg) mice were bred with PA28γ$^{-/-}$ mice to create PA28γ$^{+/-}$CoreTg mice. The PA28γ$^{+/-}$CoreTg offspring were bred with each other, and PA28γ$^{-/-}$CoreTg mice were selected by PCR using primers specific to the target sequences (Fig. 1*A*). No significant differences in body weight were observed among the 6-month-old mice, although PA28γ$^{-/-}$ mice exhibited a slight retardation of growth (Fig. 1*B*). A similar level of PA28γ expression was detected in PA28γ^{-} CoreTg and PA28γ^{-} mice (see Fig. 5*B*). The expression levels and molecular size of HCV core protein were similar in the livers of PA28γ^{-} CoreTg and PA28γ^{-} CoreTg mice (Fig. 1*C*; see also Fig. 5*B*).

PA28γ Is Required for Degradation of HCV Core Protein in the Nucleus and Induction of Liver Steatosis. HCV core protein has been detected at various sites, such as the endoplasmic reticulum, mitochondria, lipid droplets, and nucleus of cultured cell lines, as well as in hepatocytes of PA28γ^{+} CoreTg mice and hepatitis C patients

(6, 23, 24). Although HCV core protein is predominantly detected in the cytoplasm of the liver cells of PA28γ$^{+/+}$CoreTg mice, as reported in ref. 6, in the present study a clear accumulation of HCV core protein was observed in the liver cell nuclei of PA28γ$^{-/-}$CoreTg mice (Fig. 1*D*). These findings clearly indicate that at least some fraction of the HCV core protein is translocated into the nucleus and is degraded through a PA28γ-dependent pathway. Mild vacuolation was observed in the cytoplasm of the liver cells of 4-month-old PA28γ$^{+/+}$CoreTg mice, and it became more severe at 6 months, as reported in ref. 25. Hematoxylin/eosin-stained liver sections of 6-month-old PA28γ$^{+/+}$CoreTg mice exhibited severe vacuolating lesions (Fig. 2*A*), which were clearly stained with oil red O (Fig. 2*B Upper*), whereas no such lesions were detected in the livers of PA28γ$^{-/-}$CoreTg. PA28γ^{-}. or PA28γ^{-} mice at the same age. The areas occupied by the lipid droplets in the PA28γ^{+} CoreTg mouse livers were ≈10 and 2–4 times larger than those of male and female of PA28γ^{-}. PA28γ^{-} . and PA28γ^{-} CoreTg mice. respectively (Fig. 2*B Lower*). These results suggest that PA28γ is required for the induction of liver steatosis by HCV core protein in mice.

PA28γ Is Required for the Up-Regulation of SREBP-1c Transcription by HCV Core Protein in the Mouse Liver. To clarify the effects of a knockout of the PA28γ gene in PA28γ^{-} $^{+}$CoreTg mice on lipid

A

SREBP-1a   SREBP-1c   SREBP-2

B

SREBP-1c   Fatty acid synthase   Acetyl CoA carboxylase

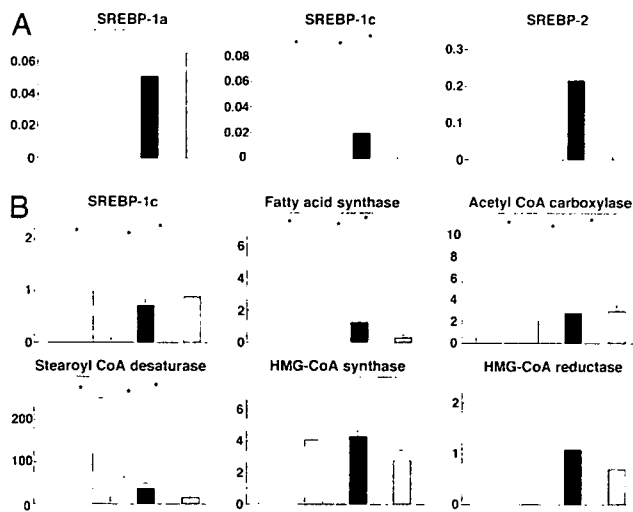Stearoyl CoA desaturase   HMG-CoA synthase   HMG-CoA reductase

Fig. 3. Transcription of genes regulating lipid biosynthesis in the mouse liver. (A) Total RNA was prepared from the livers of 2-month-old mice; and the transcription of genes encoding SREBP-1a, SREBP-1c, and SREBP-2 was determined by real-time PCR. (B) The transcription of genes encoding SREBP-1c, fatty acid synthase, acetyl-CoA carboxylase, stearoyl-CoA desaturase, HMG-CoA synthase, and HMG-CoA reductase of 6-month-old mice was measured by real-time PCR. The transcription of the genes was normalized with that of hypoxanthine phosphoribosyltransferase, and the values are expressed as relative activity ($n = 5$; $*$, $P < 0.05$; $**$, $P < 0.01$). The transcription of each gene in $PA28\gamma^{+/+}$, $PA28\gamma^{+/+}CoreTg$, $PA28\gamma^{-/-}CoreTg$, and $PA28\gamma^{-/-}$ mice is indicated by white, gray, black, and dark gray bars, respectively.

metabolism, genes related to the lipid biosyntheses were examined by real-time quantitative PCR. Transcription of SREBP-1c was higher in the livers of $PA28\gamma^{+/+}CoreTg$ mice than in those of $PA28\gamma^{+/+}$, $PA28\gamma^{-/-}$, and $PA28\gamma^{-/-}CoreTg$ mice at 2 months of age, but no such increases in SREBP-2 and SREBP-1a were observed (Fig. 3A). Although transcription of SREBP-1c and its regulating enzymes, such as acetyl-CoA carboxylase, fatty acid synthase, and stearoyl-CoA desaturase, was also enhanced in the livers of 6-month-old $PA28\gamma^{+/+}CoreTg$ mice compared with the levels in the livers of $PA28\gamma^{+/+}$, $PA28\gamma^{-/-}$, and $PA28\gamma^{-/-}CoreTg$ mice, no statistically significant differences were observed with respect to the transcription levels of cholesterol biosynthesis-related genes that are regulated by SREBP-2 (e.g., HMG-CoA synthase and HMG-CoA reductase) (Fig. 3B). These results suggest the

following: (i) the up-regulation of SREBP-1c transcription in the livers of mice requires both HCV core protein and $PA28\gamma$; and (ii) the nuclear accumulation of HCV core protein alone, which occurs because of the lack of degradation along a $PA28\gamma$-dependent proteasome pathway, does not activate the *srebp-1c* promoter.

HCV Core Protein Indirectly Potentiates *srebp-1c* Promoter Activity in an LXRα/RXRα-Dependent Manner. LXRα, which is primarily expressed in the liver, forms a complex with RXRα and synergistically potentiates *srebp-1c* promoter activity (16). Activation of RXRα by HCV core protein suggests that cellular fatty acid synthesis is modulated by the SREBP-1c pathway, although HCV core protein was not included in the transcription factor complex in the electrophoresis mobility shift assay (EMSA) (17). To analyze the effect of HCV core protein and $PA28\gamma$ on the activation of the *srebp-1c* promoter, we first examined the effect of HCV core protein on the binding of the LXRα/RXRα complex to the LXR-response element (LXRE) located upstream of the SREBP-1c gene (Fig. 4A). Although a weak shift of the labeled LXRE probe was observed by incubation with nuclear extracts prepared from 293T cells expressing FLAG-tagged LXRα and HA-tagged RXRα, a clear shift was obtained by the treatment of cells with 9-cis-retinoic acid and $22(R)$-hydroxylcholesterol, ligands for LXRα and RXRα, respectively. In contrast, coexpression of HCV core protein with LXRα and RXRα potentiated the shift of the probe irrespective of the treatment with the ligands. Addition of 500 times the amount of nonlabeled LXRE probe (competitor) diminished the shift of the labeled probe induced by the ligands and/or HCV core protein. Furthermore, coincubation of the nuclear fraction with antibody to FLAG or HA tag but not with antibody to either HCV core or $PA28\gamma$ caused a supershift of the labeled probe. These results indicate that HCV core protein does not participate in the LXRα/RXRα–LXRE complex but indirectly enhances the binding of LXRα/RXRα to the LXRE.

The activity of the *srebp-1c* promoter was enhanced by the expression of HCV core protein in 293T cells, and it was further enhanced by coexpression of LXRα/RXRα (Fig. 4B). Enhancement of the *srebp-1c* promoter by coexpression of HCV core protein and LXRα/RXRα was further potentiated by treatment with the ligands for LXRα and RXRα. The cells treated with 9-cis-retinoic acid exhibited more potent enhancement of the *srebp-1c* promoter than those treated with $22(R)$-hydroxylcholesterol. HCV core protein exhibited more potent enhancement of the *srebp-1c* promoter in cells treated with both ligands than in those treated with either ligand alone. These results suggest that HCV core protein poten-

A

Antibody / RXRα/LXRα / Core / Competitor

Ligands (-)   Ligands (+)   Ligands (-)   Ligands (+)

Core
HA-RXRα
Flag-LXRα
PA28γ

B

Fold increase

Empty vector
Core
LXRα/RXRα
LXRα/RXRα/Core

EtOH   9cisRA   22RHC   9cisRA+22RHC
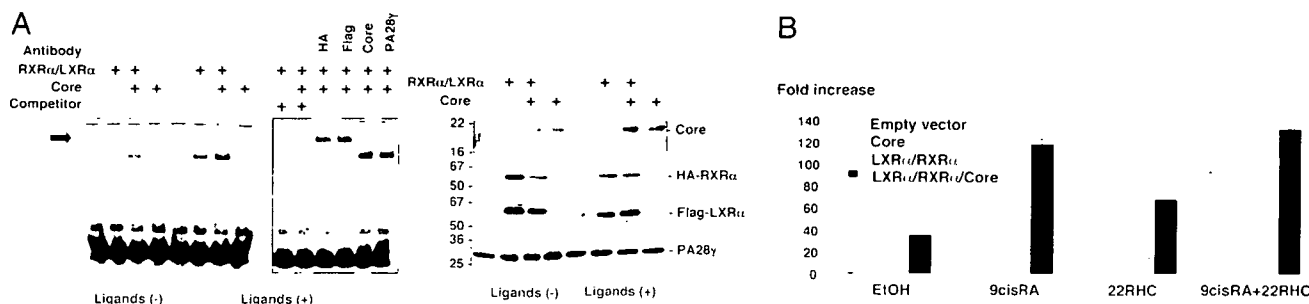
Fig. 4. Activation of the *srebp-1c* promoter by HCV core protein. (A) FLAG-LXRα and HA-RXRα were expressed in 293T cells together with or without HCV core protein. Ligands for LXRα and RXRα dissolved in ethanol [Ligands (+)] or ethanol alone [Ligands (−)] were added to the culture supernatant at 24 h posttransfection. Cells were harvested at 48 h posttransfection, and nuclear extracts were mixed with the reaction buffer for EMSA in the presence or absence of antibody (100 ng) against HA, FLAG, HCV core or $PA28\gamma$, or nonlabeled LXRE probe (Competitor). (Left) The resulting mixtures were subjected to PAGE and blotted with horseradish peroxidase/streptavidin. The mobility shift of the LXRE probe and its supershift are indicated by a gray and black arrow, respectively. (Right) Expression of HCV core, HA-RXRα, FLAG-LXRα, and $PA28\gamma$ in cells was detected by immunoblotting. (B) Effects of ligands for RXRα, 9-cis-retinoic acid (9cisRA), and for LXRα, $22(R)$-hydroxylcholesterol (22RHC), on the activation of the *srebp-1c* promoter in 293T cells expressing RXRα, LXRα, and/or HCV core protein. Ligands were added into the medium at 24 h posttransfection at a concentration of 5 μM, and the cells were harvested after 24 h of incubation.

MICROBIOLOGY

Fig. 5. PA28γ is required for HCV core-dependent activation of the *srebp-1c* promoter. (*A*) Effect of PA28γ knockdown on the LXRα/RXRα–DNA complex. FLAG-LXRα and HA-RXRα were expressed in FLC4 (control) or PA28γ-knockdown (PA28γ KD) cells together with or without HCV core protein. Cells were harvested at 48 h posttransfection, and nuclear extracts were mixed with the reaction buffer for EMSA. (*Upper*) The r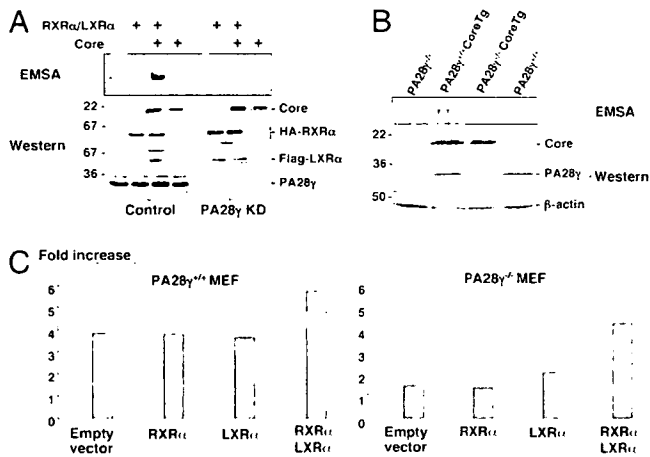esulting mixtures were subjected to PAGE and blotted with horseradish peroxidase-streptavidin. The mobility shift of the LXRE probe is indicated by an arrow. (*Lower*) Expression of HCV core, HA-RXRα, FLAG-LXRα, and PA28γ in cells was detected by immunoblotting. (*B*) Effect of PA28γ knockout on the LXRα/RXRα–DNA complex in the mouse liver. (*Upper*) Nuclear extracts were prepared from the livers of 2-month-old PA28γ⁻/⁻, PA28γ⁺/⁺CoreTg, PA28γ⁻/⁻CoreTg, and PA28γ⁺/⁺ mice and subjected to EMSA. The mobility shift of the LXRE probe is indicated by an arrow. (*Lower*) The expression of HCV core, PA28γ, and β-actin in the livers of the mice was detected by immunoblotting. (*C*) Effect of HCV core protein on *srebp-1* promoter activity in PA28γ-knockout fibroblasts. A plasmid encoding firefly luciferase under the control of the *srebp-1c* promoter was transfected into MEFs prepared from PA28γ⁺/⁺ (*Left*) or PA28γ⁻/⁻ (*Right*) mice together with a plasmid encoding a *Renilla* luciferase. An empty plasmid or plasmids encoding mouse RXRα or LXRα were also cotransfected into the cells together with (gray bars) or without (white bars) a plasmid encoding HCV core protein. Luciferase activity under the control of the *srebp-1c* promoter was determined, and it is expressed as the fold increase in relative luciferase activity after standardization with the activity of *Renilla* luciferase.

tiates *srebp-1c* promoter activity in an LXRα/RXRα-dependent manner.

HCV Core Protein Activates the *srepb-1c* Promoter in an LXRα/RXRα- and PA28γ-Dependent Manner.

To examine whether PA28γ is required for HCV core-induced enhancement of *srebp-1c* promoter activity in human liver cells, a PA28γ-knockdown human hepatoma cell line (FLC4 KD) was prepared. Enhancement of binding of the LXRE probe to LXRα/RXRα by coexpression of HCV core protein and LXRα/RXRα in FLC4 cells was diminished by knockdown of the PA28γ gene (Fig. 5*A*). Furthermore, formation of the LXRα/RXRα–LXRE complex was enhanced in the livers of PA28γ⁺ ⁺CoreTg mice but not in those of PA28γ⁻/⁻, PA28γ⁺ ⁺, or PA28γ⁻ CoreTg mice (Fig. 5*B*). The expression of the HCV core protein in the mouse embryonic fibroblasts (MEFs) of PA28γ⁺ ⁺ mice induced the activation of the mouse *srebp-1c* promoter through the endogenous expression of LXRα and RXRα (Fig. 5*C Left*). Further enhancement of the activation of the *srebp-1c* promoter by HCV core protein in PA28γ⁻ ' MEFs was achieved by the exogenous expression of both LXRα and RXRα. However, no enhancing effect of HCV core protein on *srebp-1c* promoter activity was observed in PA28γ⁻/⁻ MEFs (Fig. 5*C Right*). These results support the notion that HCV core protein enhances the activity of the *srepb-1c* promoter in an LXRα/RXRα- and PA28γ-dependent manner.

Table 1. HCC in mice at 16–18 months of age

Mouse and sex	Total no. of mice	No. of mice developing HCC	Incidence, %
PA28γ⁺/⁺CoreTg			
Male	17	5	29.4
Female	28	3	10.7
PA28γ⁺/⁻			
Male	16	0	0
Female	4	0	0
PA28γ⁻/⁻			
Male	23	0	0
Female	13	0	0
PA28γ⁻/⁻CoreTg			
Male	15	0	0
Female	21	0	0

PA28γ Plays a Crucial Role in the Development of HCC in PA28γ⁺/⁺ CoreTg Mice.

The incidence of hepatic tumors in male PA28γ⁺/⁺ CoreTg mice older than 16 months was significantly higher than that in age-matched female PA28γ⁺/⁺CoreTg mice (6). We reconfirmed here that the incidence of HCC in male and female PA28γ⁺/⁺CoreTg mice at 16–18 months of age was 29.4% (5 of 17 mice) and 10.7% (3 of 28 mice), respectively. To our surprise, however, no HCC developed in PA28γ⁻/⁻CoreTg mice (males, 15; females, 21), although, as expected, no HCC was observed in PA28γ⁺/⁻ (males, 16; females, 4) and PA28γ⁻/⁻ mice (males, 23; females, 13) (Table 1). These results clearly indicate that PA28γ plays an indispensable role in the development of HCC induced by HCV core protein.

Discussion

HCV core protein is detected in the cytoplasm and partially in the nucleus and mitochondria of culture cells and hepatocytes of transgenic mice and hepatitis C patients (6, 23, 24, 26). Degradation of HCV core protein was enhanced by deletion of the C-terminal transmembrane region through a ubiquitin/proteasome-dependent pathway (27). We previously reported (18) that PA28γ binds directly to HCV core protein and then enhances degradation of HCV core protein in the nucleus through a proteasome-dependent pathway because HCV core protein was accumulated in nucleus of human cell line by treatment with proteasome inhibitor MG132. In this work, accumulation of HCV core protein was observed in nucleus of hepatocytes of PA28γ⁻/⁻CoreTg mice (Fig. 1*D*). This result directly demonstrates that HCV core protein migrates into the nucleus and is degraded through a PA28γ-dependent pathway. However, HCV core protein accumulated in the nucleus because knockout of PA28γ gene abrogated the ability to cause liver pathology, suggesting that interaction of HCV core protein with PA28γ in the nucleus is prerequisite for the liver pathology induced by HCV core protein. We have previously shown (18) that HCV core protein is degraded through a PA28γ-dependent pathway, and Minami *et al.* (28) reported that PA28γ has a cochaperone activity with Hsp90. Therefore, degradation products of HCV core protein by means of PA28γ-dependent processing or correct folding of HCV core protein through cochaperone activity of PA28γ might be involved in the development of liver pathology. We do not know the reason why knockout of the PA28γ gene does not affect the total amount of HCV core protein in the liver of the transgenic mice. PA28γ-dependent degradation of HCV core protein may be independent of ubiquitination. as shown in SRC-3 (21). whereas knockdown of PA28γ in a human hepatoma cell line enhanced the ubiquitination of HCV core protein [ʜᴄᴠ ……………………………ʜᴄ ……………………ʜᴄᴠ …………………ᴄᴏʀᴇ], suggesting that lack of PA28γ suppresses a ubiquitin-independent degradation but enhances a ubiquitin-dependent degradation of HCV core protein. Therefore, the total amount of HCV

core protein in the liver of the mice may be unaffected by the knockout of the PA28γ gene.

Our results suggest that the interaction of HCV core protein with PA28γ leads to the activation of the *srebp-1c* promoter along an LXRα/RXRα-dependent pathway and the development of liver steatosis and HCC. HCV core protein was not included in the LXRα/RXRα–LXRE complex (Fig. 3*A*), suggesting that HCV core protein indirectly activates the *srebp-1c* promoter. Cytoplasmic HCV core protein was shown to interact with Sp110b, which is a transcriptional corepressor of RARα-dependent transcription, and this interaction leads to the sequestering of Sp110b in the cytoplasm, resulting in the activation of RARα-dependent transcription (29). The sequestration of an unidentified corepressor of the LXRα/RXRα heterodimer in the cytoplasm by HCV core protein may also contribute to the activation of the *srebp-1c* promoter. Although the precise physiological function of PA28γ-proteasome activity in the nucleus is not known, PA28γ has previously been shown (21) to regulate nuclear hormone receptors by means of the degradation of its coactivator SRC-3 and to participate in the fully Hsp90-dependent protein refolding (28). It appears reasonable to speculate that degradation or refolding of HCV core protein in a PA28γ-dependent pathway might be involved in the modulation of transcriptional regulators of various promoters, including the *srebp-1c* promoter. Saturated or monounsaturated fatty acids have been shown to enhance HCV RNA replication in Huh7 cells containing the full-length HCV replicon (7). The up-regulation of fatty acid biosynthesis by HCV core protein may also contribute to the efficient replication of HCV and to the progression of HCV pathogenesis.

Expression of HCV core protein was reported to enhance production of reactive oxygen species (ROS) (30), which leads to carbonylation of intracellular proteins (31). Enhancement of ROS production may trigger double-stranded DNA breaks and result in the development of HCC (30, 32, 33). HCV core protein could enhance the protein carbonylation in the liver of the transgenic mice in the presence but not in the absence of PA28γ (SI Fig. 7), suggesting that PA28γ is required for ROS production induced by HCV core protein. Development of HCC was observed in PA28γ$^{+/+}$CoreTg mice but not in PA28γ$^{-/-}$CoreTg mice (Table 1). Enhancement of ROS production by HCV core protein in the presence of PA28γ might be involved in the development of HCC in PA28γ$^{+/+}$CoreTg mice.

It is well known that resistant viruses readily emerge during the treatment with antiviral drugs targeting the viral protease or replicase, especially in the case of infection with RNA viruses. Therefore, antivirals targeting the host factors that are indispensable for the propagation of viruses might be an ideal target for the development of antiviral agents because of a lower rate of mutation than that of viral genome, if they have no side effects to patients. Importantly, the amino acid sequence of PA28γ of mice is identical to that of human, and mouse PA28γ is dispensable because PA28γ knockout mice exhibit no abnormal phenotype except for mild growth retardation. Therefore, PA28γ might be a promising target for an antiviral treatment of chronic hepatitis C with negligible side effects.

In summary, we observed that a knockout of the PA28γ gene from PA28γ$^{+/+}$CoreTg mice induced the accumulation of HCV core protein in the nucleus and disrupted the development of both steatosis and HCC. Activation of the *srebp-1c* promoter was up-regulated by HCV core protein both *in vitro* and *in vivo* through a PA28γ-dependent pathway, suggesting that PA28γ plays a crucial role in the development of liver pathology induced by HCV infection.

Materials and Methods

Histology and immunohistochemistry, real-time PCR, and detection of proteins modified by ROS are discussed in *SI Materials and Methods*.

Plasmids and Reagents. Human PA28γ cDNA was isolated from a human fetal brain library (18). The gene encoding HCV core protein was amplified from HCV strain J1 (genotype 1b) (34) and cloned into pCAG-GS (35). Mouse cDNAs of RXRα and LXRα were amplified by PCR from the total cDNAs of the mouse liver. The RXRα and LXRα genes were introduced into pEF-FLAGGspGBK (36) and pcDNA3.1 (Invitrogen, Carlsbad, CA), respectively. The targeting fragment for human PA28γ knockdown (GGATCCGGTGGATCAGGAAGTGAAGTTCAAGAGA-CTTCACTTCCTGATCCACCTTTTTTGGAAAAGCTT) was introduced into the BamHI and HindIII sites of pSilencer 4.1 U6 hygro vector (Ambion, Austin, TX). Mouse anti-FLAG (M2) and mouse anti-β-actin antibodies were purchased from Sigma (St. Louis, MO). Rabbit polyclonal antibody against synthetic peptides corresponding to amino acids 70–85 of PA28γ was obtained from AFFINITI (Exeter, U.K.). Horseradish peroxidase-conjugated goat anti-mouse and anti-rabbit IgGs were purchased from ICN Pharmaceuticals (Aurora, OH). Rabbit anti-HCV core protein was prepared by immunization with recombinant HCV core protein (amino acids 1-71), as described in ref. 24. Mouse monoclonal antibody to HCV core protein was kindly provided by S. Yagi (37). The plasmid for expression of HA-tagged ubiquitin was described in ref. 27.

Preparation of PA28γ-Knockout HCV CoreTg Mice. The generation of C57BL/6 mice carrying the gene encoding HCV core protein genotype 1b line C49 and that of PA28γ$^{-/-}$ mice have been reported previously (22, 25). Both strains were crossbred with each other to create PA28γ$^{-/-}$CoreTg mice. PA28γ$^{-/-}$CoreTg mice were identified by PCR targeted at the PA28γ or HCV core gene (22, 25). Using 1 μg of genomic DNA obtained from the mouse tail, the PA28γ gene was amplified by PCR with the following primers: sense, PA28-3 (AGGTGGATCAGGAAGTGAAGCTCAA); and antisense, PA28γ-5cr (CACCTCACTTGTGATCCGCTCTCT-GAAAGAATCAACC). The targeted sequence for the PA28γ-knockout mouse was detected by PCR using the PA28-3 primer and the PAKO-4 primer (TGCAGTTCATTCAGGGCACCGGA-CAG). The transgene encoding HCV core protein was detected by PCR as described in ref. 25. The expression of PA28γ and HCV core protein in the livers of 6-month-old mice was confirmed by Western blotting with mouse monoclonal antibody to HCV core protein, clone 11-10, and rabbit antibody to PA28γ. Mice were cared for according to the institutional guidelines. The mice were given ordinary feed, CRF-1 (Charles River Laboratories, Yokohama, Japan), and they were maintained under specific pathogen-free conditions.

All animal experiments conformed to the Guidelines for the Care and Use of Laboratory Animals, and they were approved by the Institutional Committee of Laboratory Animal Experimentation (Research Institute for Microbial Diseases, Osaka University).

Preparation of Mouse Embryonic Fibroblasts. MEFs were prepared as described in ref. 22. MEFs were cultured at 37°C under an atmosphere of 5% CO_2 in Dulbecco's modified Eagle's medium (Sigma) supplemented with 10% FBS, penicillin, streptomycin, sodium pyruvate, and nonessential amino acids.

Transfection and Immunoblotting. Plasmid vectors were transfected into the MEFs and 293T cells by liposome-mediated transfection by using Lipofectamine 2000 (Invitrogen). The amount of HCV core protein in the liver tissues was determined by an ELISA as described in ref. 37. The cell lysates were subjected to SDS/PAGE (12.5% gel), and they were then transferred onto PVDF membranes. Proteins on the membranes were treated with specific antibody and Super Signal Femto (Pierce, Rockford, IL). The results were then visualized by using an LAS3000 imaging system (Fuji Photo Film, Tokyo, Japan). The method of immunoprecipitation test is described in ref. 18.

MICROBIOLOGY

Reporter Assay for *srebp-1c* Promoter Activity. The genomic DNA fragment encoding the *srebp-1c* promoter region (located from residues −410 to +24) was amplified from a mouse genome. The fragment was introduced into the KpnI and HindIII sites of pGL3-Basic (Promega, Madison, WI), and it was designated as pGL3-srebp-1cPro. The plasmids encoding RXRα and LXRα were transfected into MEFs together with pGL3-srebp-1cPro and a control plasmid encoding *Renilla* luciferase (Promega). The total DNA for transfection was normalized by the addition of empty plasmids. Cells were harvested at 24 h posttransfection. The ligand of RXRα, 9-*cis*-retinoic acid (Sigma), and that of LXRα, 22(*R*)-hydroxylcholesterol (Sigma) were added at a final concentration of 5 μM each to the culture medium of 293T cells transfected with pGL3-srebp-1cPro together with expression plasmids encoding RXRα, LXRα, and HCV core protein at 24 h posttransfection. Cells were harvested 24 h after treatment. Luciferase activity was measured by using the dual-luciferase reporter assay system (Promega). Firefly luciferase activity was standardized with that of *Renilla* luciferase, and the results are expressed as the fold increase in relative luciferase units.

Electrophoresis Mobility Shift Assay (EMSA). EMSA was carried out by using a LightShift Chemiluminescent EMSA kit (Pierce) according to the manufacturer's protocol. Nuclear extract of the cell lines and liver tissue was prepared with an NE-PER nuclear and cytoplasmic extraction reagent kit (Pierce). Briefly, double-stranded oligonucleotides for EMSA were prepared by annealing both strands of each LXRE of the *srebp-1c* promoter (5′-GGACGCCCGCTAGTAACCCCGGC-3′) (16). Both strands were labeled at the 5′ ends with biotin. The annealed probe was incubated for 20 min on ice with nuclear extract (3 μg of protein) in a reaction buffer containing 10 mM Tris·HCl (pH 7.5), 50 mM KCl, 1 mM DTT, 0.05 μg/μl poly(dI-dC), 2.5% glycerol, 0.05% Nonidet P-40, and 0.1 nM labeled probe, with or without 1 mM nonlabeled probe. The resulting mixture was subjected to PAGE (5% gel) at 120 V for 30 min in 0.5× TBE. The DNA–protein complex was transferred to a Hybond N+ membrane (Amersham, Piscataway, NJ), incubated with horseradish peroxidase-conjugated streptavidin, and visualized by using an LAS3000 imaging system.

Statistical Analysis. The results are expressed as the mean ± SD. The significance of differences in the means was determined by Student's *t* test.

1. Wasley A, Alter MJ (2000) *Semin Liver Dis* 20:1–16.
2. Bach N, Thung SN, Schaffner F (1992) *Hepatology* 15:572–577.
3. Lefkowitch JH, Schiff ER, Davis GL, Perrillo RP, Lindsay K, Bodenheimer HC. Jr., Balart LA, Ortego TJ. Payne J, Dienstag JL. *et al.* (1993) *Gastroenterology* 104:595–603.
4. Barba G, Harper F. Harada T. Kohara M. Goulinet S. Matsuura Y. Eder G. Schaff Z, Chapman MJ. Miyamura T. Brechot C (1997) *Proc Natl Acad Sci USA* 94:1200–1205.
5. Hope RG. McLauchlan J (2000) *J Gen Virol* 81:1913–1925.
6. Moriya K, Fujie H. Shintani Y, Yotsuyanagi H, Tsutsumi T, Ishibashi K, Matsuura Y. Kimura S. Miyamura T. Koike K (1998) *Nat Med* 4:1065–1067.
7. Kapadia SB. Chisari FV (2005) *Proc Natl Acad Sci USA* 102:2561–2566.
8. Su AI, Pezacki JP, Wodicka L, Brideau AD. Supekova L. Thimme R, Wieland S. Bukh J, Purcell RH, Schultz PG. Chisari FV (2002) *Proc Natl Acad Sci USA* 99:15669–15674.
9. Wang C, Gale M, Jr. Keller BC, Huang H. Brown MS. Goldstein JL, Ye J (2005) *Mol Cell* 18:425–434.
10. Horton JD, Shimomura I. Brown MS, Hammer RE. Goldstein JL, Shimano H (1998) *J Clin Invest* 101:2331–2339.
11. Pai JT, Guryev O. Brown MS, Goldstein JL (1998) *J Biol Chem* 273:26138–26148.
12. Shimano H, Horton JD. Hammer RE, Shimomura I. Brown MS, Goldstein JL (1996) *J Clin Invest* 98:1575–1584.
13. Shimano H. Horton JD, Shimomura I, Hammer RE. Brown MS. Goldstein JL (1997) *J Clin Invest* 99:846–854.
14. Shimano H. Shimomura I, Hammer RE, Herz J. Goldstein JL, Brown MS. Horton JD (1997) *J Clin Invest* 100:2115–2124.
15. Repa JJ. Liang G, Ou J. Bashmakov Y. Lobaccaro JM. Shimomura I. Shan B. Brown MS. Goldstein JL. Mangelsdorf DJ (2000) *Genes Dev* 14:2819–2830.
16. Yoshikawa T, Shimano H. Amemiya-Kudo M. Yahagi N. Hasty AH. Matsuzaka T. Okazaki H. Tamura Y. Iizuka Y, Ohashi K. *et al.* (2001) *Mol Cell Biol* 21:2991–3000.
17. Tsutsumi T. Suzuki T. Shimoike T. Suzuki R. Moriya K, Shintani Y. Fujie H. Matsuura Y. Koike K, Miyamura T (2002) *Hepatology* 35:937–946.
18. Moriishi K, Okabayashi T, Nakai K. Moriya K, Koike K. Murata S, Chiba T. Tanaka K. Suzuki R, Suzuki T. *et al.* (2003) *J Virol* 77:10237–10249.
19. Masson P. Andersson O. Petersen UM, Young P (2001) *J Biol Chem* 276:1383–1390.
20. Li J, Rechsteiner M (2001) *Biochimie* 83:373–383.
21. Li X. Lonard D, Jung SY. Malovannaya A. Feng Q, Qin J. Tsai SY, Tsai M. O'Malley BW (2006) *Cell* 124:381–392.
22. Murata S, Kawahara H, Tohma S. Yamamoto K, Kasahara M. Nabeshima Y. Tanaka K, Chiba T (1999) *J Biol Chem* 274:38211–38215.
23. Falcon V. Acosta-Rivero N. Chinea G. Gavilondo J. de la Rosa MC. Menendez I, Duenas-Carrera S. Vina A, Garcia W, Gra B. *et al.* (2003) *Biochem Biophys Res Commun* 305:1085–1090.
24. Suzuki R. Sakamoto S, Tsutsumi T. Rikimaru A, Tanaka K, Shimoike T. Moriishi K. Iwasaki T. Mizumoto K, Matsuura Y. *et al.* (2005) *J Virol* 79:1271–1281.
25. Moriya K, Yotsuyanagi H. Shintani Y. Fujie H, Ishibashi K. Matsuura Y, Miyamura T. Koike K (1997) *J Gen Virol* 78:1527–1531.
26. Yasui K, Wakita T. Tsukiyama-Kohara K. Funahashi SI, Ichikawa M. Kajita T. Moradpour D, Wands JR, Kohara M (1998) *J Virol* 72:6048–6055.
27. Suzuki R. Tamura K. Li J, Ishii K. Matsuura Y, Miyamura T. Suzuki T (2001) *Virology* 280:301–309.
28. Minami Y. Kawasaki H. Minami M, Tanahashi N, Tanaka K, Yahara I (2000) *J Biol Chem* 275:9055–9061.
29. Watashi K, Hijikata M. Tagawa A, Doi T. Marusawa H. Shimotohno K (2003) *Mol Cell Biol* 23:7498–7509.
30. Machida K. Cheng KT. Lai CK, Jeng KS, Sung VM. Lai MM (2006) *J Virol* 80:7199–7207.
31. Nystrom T (2005) *EMBO J* 24:1311–1317.
32. Bromberg JF, Wrzeszczynska MH. Devgan G. Zhao Y. Pestell RG, Albanese C, Darnell JE. Jr (1999) *Cell* 98:295–303.
33. Carballo M. Conde M, El Bekay R, Martin-Nieto J, Camacho MJ, Monteseirin J, Conde J, Bedoya FJ. Sobrino F (1999) *J Biol Chem* 274:17580–17586.
34. Aizaki H. Aoki Y. Harada T, Ishii K, Suzuki T. Nagamori S. Toda G, Matsuura Y. Miyamura T (1998) *Hepatology* 27:621–627.
35. Niwa H. Yamamura K. Miyazaki J (1991) *Gene* 108:193–199.
36. Huang DC. Cory S. Strasser A (1997) *Oncogene* 14:405–414.
37. Aoyagi K. Ohuc C. Iida K. Kimura T. Tanaka E. Kiyosawa K, Yagi S (1999) *J Clin Microbiol* 37:1802–1808.

Hepatitis C Virus Nonstructural Protein 5A Modulates the Toll-Like Receptor-MyD88-Dependent Signaling Pathway in Macrophage Cell Lines[▽]

Takayuki Abe,[1] Yuuki Kaname,[1] Itsuki Hamamoto,[1][†] Yoshimi Tsuda,[1][‡] Xiaoyu Wen,[1]
Shuhei Taguwa,[1] Kohji Moriishi,[1] Osamu Takeuchi,[2] Taro Kawai,[2] Tatsuya Kanto,[3,4]
Norio Hayashi,[3] Shizuo Akira,[2] and Yoshiharu Matsuura[1]*

Department of Molecular Virology,[1] and Department of Host Defense,[2] Research Institute for Microbial Diseases, and Department of Gastroenterology and Hepatology,[3] and Department of Dendritic Cell Biology and Clinical Applications,[4] Graduate School of Medicine, Osaka University, Osaka, Japan

Received 27 March 2007/Accepted 6 June 2007

Hepatitis C virus (HCV) infection induces a wide range of chronic liver injuries; however, the mechanism through which HCV evades the immune surveillance system remains obscure. Blood dendritic cells (DCs) play a pivotal role in the recognition of viral infection and the induction of innate and adaptive immune responses. Several reports suggest that HCV infection induces the dysfunction of DCs in patients with chronic hepatitis C. Toll-like receptor (TLR) has been shown to play various roles in many viral infections; however, the involvement of HCV proteins in the TLR signaling pathway has not yet been precisely elucidated. In this study, we established mouse macrophage cell lines stably expressing HCV proteins and determined the effect of HCV proteins on the TLR signaling pathways. Immune cells expressing NS3, NS3/4A, NS4B, or NS5A were found to inhibit the activation of the TLR2, TLR4, TLR7, and TLR9 signaling pathways. Various genotypes of NS5A bound to MyD88, a major adaptor molecule in TLR, inhibited the recruitment of interleukin-1 receptor-associated kinase 1 to MyD88, and impaired cytokine production in response to TLR ligands. Amino acid residues 240 to 280, previously identified as the interferon sensitivity-determining region (ISDR) in NS5A, interacted with the death domain of MyD88, and the expression of a mutant NS5A lacking the ISDR partially restored cytokine production. These results suggest that the expression of HCV proteins modulates the TLR signaling pathway in immune cells.

Hepatitis C virus (HCV) belongs to the family *Flaviviridae* and possesses a positive, single-stranded RNA genome that encodes a single polyprotein composed of approximately 3,000 amino acids. HCV polyprotein is processed by host and viral proteases, resulting in 10 viral proteins. Viral structural proteins, including the capsid protein and two envelope proteins, are located in the N-terminal one-third of the polyprotein, followed by nonstructural proteins. HCV infects 170 million people worldwide and frequently leads to cirrhosis and hepatocellular carcinoma (36). In over one-half of patients, acute infection evolves into a persistent carrier state, presumably due to the ability of HCV to incapacitate the activation of the host immune mechanisms. Dendritic cells (DCs) are one type of potent antigen-presenting cell in vivo and play a crucial role in the enhancement and regulation of cell-mediated immune reactions. Since DCs express various costimulatory and/or adhesion molecules, they can activate even naïve T cells in a primary response. The role of the response of HCV antigen-specific T cells in viral clearance or persistence has been in-

vestigated extensively in both humans and chimpanzees (6, 27, 48, 51). These studies suggest that acute HCV infections followed by viral clearance are associated with a high frequency of HCV-specific CD4^{+} and CD8^{+} T-cell responses that can persist (27, 51), while chronic HCV infections are characterized by weak and restricted CD4^{+} and CD8^{+} T-cell responses that are not sustained (51).

Toll-like receptors (TLRs) are membrane-bound receptors that can be activated by the binding of molecular structures conserved among families of microbes. More than 10 different TLRs have been identified to date (2). They are highly conserved among mammals and are expressed in a variety of cell types. TLR binding and stimulation by pathogen-associated molecules is followed by a cascade of intracellular events that culminate in the expression of multiple genes (2). TLR signaling is mediated primarily by the adaptor protein myeloid differentiation factor 88 (MyD88), which triggers the activation of transcription factors, such as NF-κB, that are essential for the expression of proinflammatory cytokine genes (2). This pathway also leads to the potent production of type 1 interferon (IFN) through the activation of IFN regulatory factor 7 (IRF7) upon stimulation of TLR7 or TLR9 (22). In contrast, Toll/interleukin-1 (IL-1) receptor homology domain-containing adaptor-inducing IFN-β (TRIF/TICAM-1) mediates the production of type I IFNs primarily through the activation of IRF3 in response to TLR3 or TLR4 stimulation (2). Type 1 IFN induces the maturation of DCs by increasing both the expression of costimulatory molecules such as CD80, CD86, and CD40 and antigen presentation via major histocompatibility

complex class I in addition to classical endogenous antigen presentation; it also facilitates the cross-presentation of viral antigens. A cumulative report has shown that DC activation via TLR signaling is a prerequisite for the subsequent induction of vigorous T-cell responses (42). Some viral proteins have been shown to inhibit the TLR-dependent signaling pathway through interactions with the downstream adaptor molecules, suggesting that the alteration of TLR-mediated signals is one of the mechanisms of virus-induced immune modulation (49). Dysfunction of DCs in patients with chronic HCV infection due to immaturation caused by the direct infection of DCs by HCV or by interactions with HCV proteins has been reported previously (4, 21). On the other hand, there have also been contrasting reports suggesting a lack of impairment of DC function in both chimpanzees and humans chronically infected with HCV (26, 32). Thus, at present, alterations in the TLR signaling pathway in the immune cells of patients with chronic hepatitis C virus infection are not well understood.

In the present study, we examined the effect of HCV proteins on TLR function in murine macrophage cell lines stably expressing HCV proteins. The expression of NS3, NS3/4A, NS4B, or NS5A was found to impair the activation of the TLR signaling pathways, and NS5A interacted with MyD88 through the IFN sensitivity-determining region (ISDR) and impaired cytokine production. To the best of our knowledge, this is the first demonstration of NS5A as an immunomodulator of TLR signaling pathways through the direct interaction with an adaptor molecule in immune cells.

MATERIALS AND METHODS

Cell culture. Human embryonic kidney 293T cells and mouse macrophage RAW264.7 cells were maintained in Dulbecco's modified Eagle's medium (Sigma, St. Louis, MO) containing 10% fetal calf serum. All cells were cultured at 37°C in a humidified atmosphere with 5% CO_2.

Plasmids and viruses. DNA fragments encoding each of the HCV structural and nonstructural proteins were generated from a full-length cDNA clone of genotype 1b strain J1 (1) by PCR using *Pfu* Turbo DNA polymerase (Stratagene, La Jolla, CA). The fragments were cloned into pCAGGs-puro/N-Flag, in which the sequence encoding a Flag tag is inserted at the 5′ terminus of the cloning site of pCAGGs-puro (37). A protease-deficient NS3/4A mutant with Ser[159] replaced with Ala (S139A) was generated by the method of splicing by overlap extension and cloned into pCAGGs-puro. NS5A genes were amplified by PCR from HCV clones of strains of J1 (genotype 1b), H77c (genotype 1a, kindly provided by J. Bukh). and JFH1 (genotype 2a, kindly provided by T. Wakita) and cloned into pcDNA3.1Flag/HA (38). The NS5A deletion mutants were prepared as described previously (16). DNA fragments encoding a human MyD88, human Toll–IL-1 receptor domain-containing adapter protein (TIRAP), and human TRIF-related adapter molecule (TRAM) were amplified by reverse transcription-PCR from total RNA of THP-1 cells and cloned into pcDNA3.1-C-Myc-His (Invitrogen, Carlsbad, CA) and pcDNA3.1Flag/HA. Murine IPS-1 (mIPS-1) was amplified from total RNA of RAW264.7 cells by reverse transcription-PCR and cloned into pcDNA3.1Flag/HA. Human MyD88 deletion mutants and a mIPS-1 mutant with Cys[508] replaced by Ala (C508A) were generated by the method of splicing by overlap extension and cloned into pcDNA3.1Flag/HA. pCMVI-RAK1-myc and pCMVIRAK4-myc. encoding IL-1 receptor-associated kinase 1 (IRAK-1) and IRAK-4, respectively, were prepared as described previously (53). pEFBossTICAM-1-HA was kindly provided by T. Seya (44). All PCR products were confirmed by sequencing by using an ABI PRSM 310 genetic analyzer (Applied Biosystems, Tokyo, Japan). Vesicular stomatitis virus (VSV) (Indiana strain, NCP12.1) (19) was kindly provided by M. A. Whitt.

Establishment of stable cell lines expressing HCV proteins. pCAGGs-puro/N-Flag plasmids encoding HCV proteins were transfected into RAW264.7 cells by liposome-mediated transfection using Lipofectamine 2000 (Invitrogen) and selected with 10 μg/ml of puromycin (InvivoGen, San Diego, CA). After about 2 to 3 weeks of selection, several clones were isolated, and cell lysates of each clone were immunoblotted with each of specific mouse anti-HCV antibody (1) or

anti-Flag M2 mouse monoclonal antibody (Sigma). Macrophage cell lines stably expressing HCV proteins and a control cell line obtained by transfection with an empty pCAGGs-puro vector were maintained in the presence of puromycin (10 μg/ml) throughout the experiments.

Immunoprecipitation and immunoblotting. Cells were seeded onto a six-well tissue culture plate 24 h before transfection. The plasmids were transfected by the lipofection method, and the cells were harvested at 48 h posttransfection. washed three times with 1 ml of ice-cold phosphate-buffered saline (PBS), and suspended in 0.4 ml lysis buffer containing 20 mM Tris-HCl (pH 7.4), 135 mM NaCl. 1% Triton X-100, 10% glycerol, and protease inhibitor cocktail tablets (Roche Molecular Biochemicals, Mannheim, Germany). Cell lysates were incubated for 30 min at 4°C and centrifuged at 14,000 × g for 15 min at 4°C. The supernatant was immunoprecipitated with 1 μg of mouse monoclonal anti-Flag M2, anti-hemagglutinin (HA) 16B12 (HA.11: BabCO, Richmond, CA), or anti-hexahistidine (Santa Cruz Biotechnology, Santa Cruz, CA) antibody and 10 μl of protein G-Sepharose 4B Fast Flow beads (Amersham Pharmacia Biotech, Franklin Lakes, NJ) at 4°C for 90 min. The immunocomplex was precipitated with the beads by centrifugation at 5,000 × g for 1 min and then washed five times with 0.4 ml of 20 mM Tris-HCl (pH 7.4) containing 135 mM NaCl and 0.05% Tween 20 (TBST buffer) by centrifugation. The proteins binding to the beads were boiled in 20 μl of sample buffer and then subjected to sodium dodecyl sulfate–12.5% polyacrylamide gel electrophoresis and transferred onto polyvinylidene difluoride membranes (Millipore. Tokyo, Japan). The membranes were blocked with TBST containing 5% skim milk at room temperature for 1 h; incubated with mouse monoclonal anti-Flag M2, anti-HA 16B12, or anti-hexa-histidine monoclonal antibody at room temperature for 1 h; and then incubated with horseradish peroxidase-conjugated anti-mouse immunoglobulin G (IgG) antibody at room temperature for 1 h. The cell lines (2 × 10⁶ cells/well) were stimulated with various doses of lipopolysaccharide (LPS) derived from *Salmonella enterica* serovar Minnesota (Re-595) (Sigma), peptidoglycans (PGN) derived from *Staphylococcus aureus* (Sigma). R-837 (InvivoGen), or phosphorothioate-stabilized mouse CpG (mCpG) oligodeoxynucleotides (ODN1668) (TCC-ATG-ACG-TTC-CTG-ATG-CT) (Invitrogen) for the times indicated, and the phosphorylation status of extracellular signal-regulated kinase (ERK) was determined by immunoblotting using antibodies specific to ERK1/2 or phosphorylated ERK1/2 (T202/Y204) (Cell Signaling Technology, Inc., Beverly, MA). Cells (1 × 10⁶ cells/well) were treated with various doses of mouse IFN-α (PBL Biomedical Laboratories, New Brunswick, NJ) or VSV for 24 h, and the phosphorylation status of double-stranded RNA-dependent protein kinase (PKR) and signal transducer and activator of transcription 1 (STAT1) was determined by immunoblotting using antibodies specific to STAT1 (Cell Signaling). phosphorylated STAT1 (Cell Signaling), or phosphorylated PKR (BioSource International, Inc., Camarillo. CA). The immune complexes were visualized with Super Signal West Femto substrate (Pierce, Rockford, IL) and detected by using an LAS-3000 image analyzer system (Fujifilm, Tokyo, Japan).

Cytokine production and enzyme-linked immunosorbent assay (ELISA). To evaluate cytokine production in macrophage cell lines expressing HCV proteins, cells were seeded onto 96-well plates at a concentration of 1 × 10⁵ cells/well and stimulated with various doses of LPS, PGN, R-837, or mCpG. After 24 h of incubation, culture supernatants were collected, and IL-6 production was determined by using an OptEIA mouse IL-6 set purchased from BD Pharmingen (San Diego, CA).

Real-time PCR. The cell lines (3 × 10⁶ cells/well) were stimulated with R-837, LPS, PGN, mCpG. VSV. and polyinosine-poly(C) [poly(I:C)] (Invivogen) for the times indicated, and the expression of mRNA of cytokines, chemokines, and TLR genes was determined by real-time PCR. Total RNA was prepared from the macrophage cell lines using an RNeasy Mini kit (QIAGEN). First-strand cDNA was synthesized using a ReverTra Ace (TOYOBO. Japan) and oligo(dT)₂₀ primer. Each cDNA was estimated by Platinum SYBR Green qPCR SuperMix UDG (Invitrogen) according to the manufacturer's protocol. Fluorescent signals were analyzed by using an ABI PRISM 7000 apparatus (Applied Biosystems). Mouse Ccl2, IFN-β, IFN-α4. and IL-1-α genes were amplified with primer pairs 5′-GCATCCACGTGTTGGCTCA-3′ and 5′-CTCCAGCCTACTC ATTGGGATCA-3′. 5′-ACACCAGCCTGGCTTCCATC-3′ and 5′-TTGGAG CTGGAGCTGCTTATAGTTG-3′. 5′-AGCCTTGACACTCCTGGTACAAAT G-3′ and 5′-TGGGTCAGCTCACTCAGGACA-3′. 5′-GCTCAAGCCATCCT TGTGCTAA-3′ and 5′-CATTGAGCTGATGGAGGTC 3′. and 5′-TTGGTTA AATGACCTGCAACAGGA-3′ and 5′-AGGTCGGTCTCACTACCTGTGAT G-3′. respectively. The mouse TLR2. TLR3, TLR4, TLR7, TLR9, and GAPDH (glyceraldehyde-3-phosphate dehydrogenase) genes were amplified using primer pairs 5′-AGCTCTTTGGCTCTTCTG-3′ and 5′-AGAACTGGGGGATATGC-3′. 5′ AAATCCTTGCGTTGCGAAGTG-3′ and 5′ TCAGTTGGGCGTTGTT CAAGAG-3′. 5′-GCCTCGAATCCTGAGCAAACA-3′ and 5′-CTTCTGCCC GGTAAGGTCCA-3′. 5′-TCTGCAGGAGCTCTGTCCTTGA-3′ and 5′-CAAG GCATGTCCTAGGTGGTGA-3′. 5′-ACCAATGGCACCCTGCCTAA-3′ and 5′-
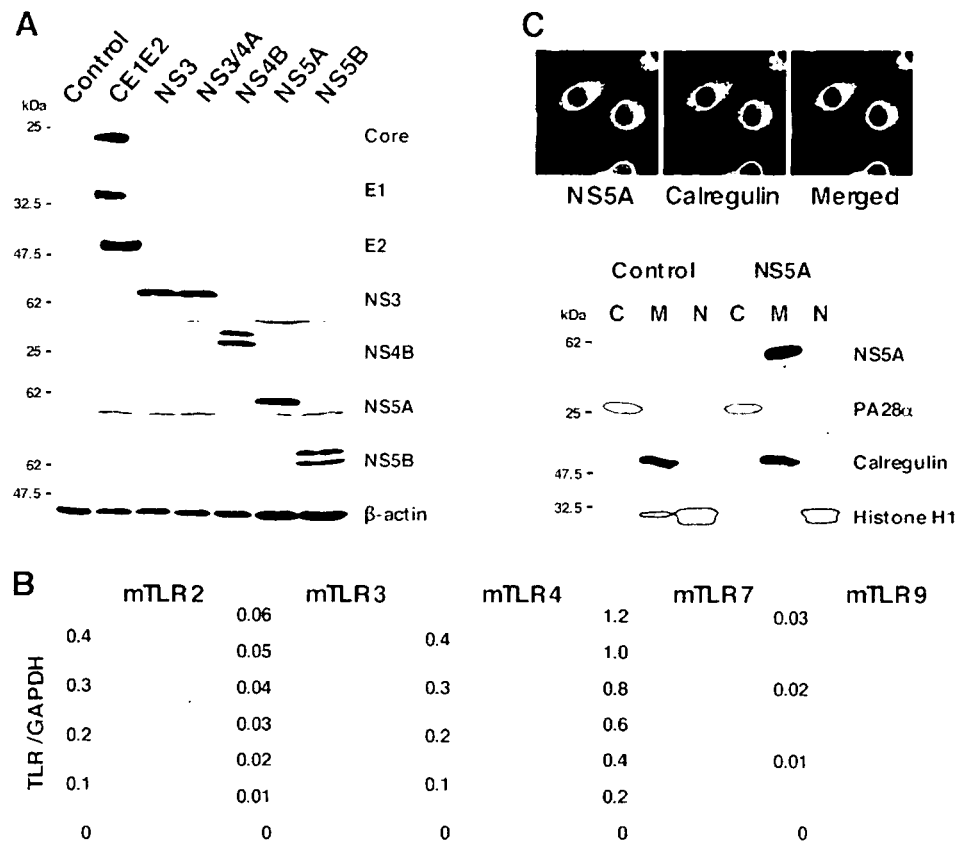
FIG. 1. Establishment of stable macrophage cell lines expressing HCV proteins. (A) Cell lysates were prepared from macrophage cell lines expressing each of the HCV proteins (4 × 10⁶ cells) and immunoblotted with antibodies against HCV proteins or β-actin. (B) Total RNA was extracted from macrophage cell lines expressing NS5A (gray bars) or control (white bars), and the expression of mRNA of TLRs was determined by real-time PCR. (C) The subcellular localization of NS5A was examined by confocal microscopy. Cells were fixed with 4% paraformaldehyde–PBS, permeabilized with 0.5% Triton X-100, and stained with specific antibodies. Cells expressing NS5A or control cells were extracted into cytosol (C), membrane-organelle (M), and nuclear (N) fractions. Each fraction was concentrated and subjected to immunoblotting with specific antibodies. PA28α, calregulin, and histone H1 were used as markers for cytosol, membrane-organelle, and nuclear fractions, respectively.

CGTCTTGAGAATGTTGTGGCTGA-3', and 5'-ACCACAGTCCATGCCATC AC-3' and 5'-TCCACCACCCTGTTGCTGTA-3', respectively. The expression of mRNAs of each of the chemokines, cytokines, and TLR was normalized with that of GAPDH mRNA.

Immunofluorescence microscopy and subcellular localization of HCV proteins in stable macrophage cell lines. Cells were seeded onto an eight-well chamber slide at 1.5 × 10⁴ cells per well, washed twice with PBS, fixed with PBS containing 4% paraformaldehyde at 18 h of cultivation, and permeabilized with PBS containing 0.5% Triton X-100 at 15 min. The cells were then incubated at 4°C for 1 h with 1 μg of mouse anti-NS5A antibody (Austral Biologicals, San Ramon, CA) or rabbit polyclonal antibody against calregulin (Santa Cruz Biotechnology) in PBS containing 10% fetal calf serum (PBSF) and then incubated at room temperature for 1 h with 0.5 μg of Alexa Fluor 488-conjugated anti-mouse IgG (Molecular Probes) or Alexa Fluor 594-conjugated anti-rabbit IgG (Molecular Probes) after three washes with PBSF. After extensive washing with PBSF, the samples were examined with a FluoView FV1000 laser scanning confocal microscope (Olympus, Japan). To confirm the subcellular localization of the HCV proteins in the macrophage cell lines, each stable cell line was fractionated with a Subcellular Proteome Extraction kit (Calbiochem, Darmstadt, Germany). Stepwise extraction resulted in four distinct fractions, which contained primarily cytosolic, membrane-organelle, nuclear, and cytoskeleton proteins, respectively. Each fraction was concentrated by Microcon (Millipore) and subjected to immunoblotting. PA28α (Biomol International, Plymouth Meeting, PA), calregulin, and histone H1 (Santa Cruz Biotechnology) were used as cytoplasmic, membrane, and nuclear markers, respectively.

RESULTS

Establishment of macrophage cell lines stably expressing HCV proteins. To examine the effect of HCV proteins on the TLR function of immune cells, we established murine macrophage cell lines stably expressing HCV structural or nonstructural proteins. We selected mouse macrophage RAW264.7 cells due to their high level of expression of various TLRs (3) and their high sensitivity to stimulation with TLR ligands. Processed HCV structural and nonstructural proteins were detected in each of the cell lines by immunoblot analyses using specific monoclonal antibodies (Fig. 1A). To examine the effect of HCV proteins on TLR expression in macrophage cell lines, the mRNA of TLRs in cells expressing NS5A was determined by real-time PCR (Fig. 1B). Although slight reductions in TLR2, TLR3, and TLR4 or enhancement of TLR7 and TLR9 was observed, a substantial amount of mRNA of the examined TLRs was detected in the cell lines expressing NS5A and other HCV proteins (data not shown). To determine the subcellular localization of HCV proteins in macrophage cell lines, the expression of HCV proteins was examined by con-
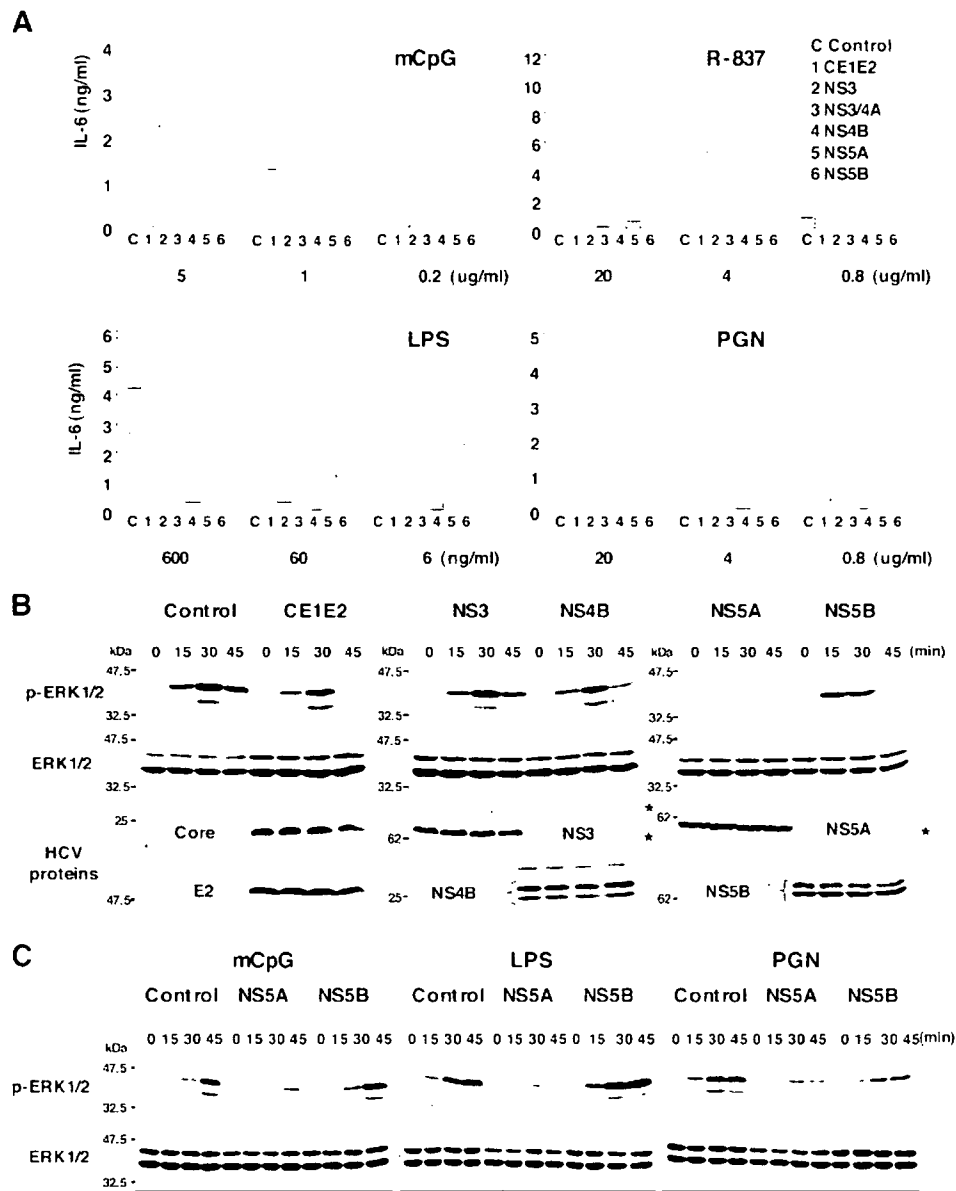
FIG. 2. Expression of HCV nonstructural proteins modulates IL-6 production and MAPK cascades through the TLR-dependent signaling pathway in macrophage cell lines. (A) Cells were seeded onto 96-well plates (1 × 10^5 cells/well) and stimulated with the indicated amounts of mCpG, R-837, LPS, or PGN. After 24 h of stimulation, IL-6 production in the culture supernatants was determined by sandwich ELISA. Data are shown as means ± standard deviations (SD). (B) Cells (2 × 10^6 cells/well) were stimulated with 10 μg/ml of R-837 for the times indicated, and ERK1/2 phosphorylation was determined by immunoblotting with antibodies to ERK and phosphorylated ERK (p-ERK). Asterisks indicate nonspecific bands. (C) Cells (2 × 10^6 cells/well) were stimulated with 10 μg/ml of mCpG, 25 ng/ml of LPS, or 10 μg/ml of PGN for the times indicated, and ERK1/2 phosphorylation was determined by immunoblotting.

focal microscopy and cell fractionation (Fig. 1C). HCV NS5A was colocalized with the endoplasmic reticulum marker calregulin in the macrophage cell line as reported previously for human hepatoma cell lines (47). Other HCV proteins exhibited similar localization with NS5A (data not shown). To further confirm the subcellular localization of NS5A proteins, cytoplasmic, membrane-organelle, and nuclear fractions of the cell line expressing NS5A were analyzed by Western blotting. NS5A was detected mainly in the membrane-organelle fraction.

Expression of HCV NS3, NS3/4A, NS4B, or NS5A modulates the TLR-dependent signaling pathway in macrophage cell lines. In order to determine the effect of the expression of HCV proteins on the TLR signaling pathway in macrophage cell lines, we examined the ability of HCV proteins to inhibit NF-κB activation via stimulation with various TLR ligands. The macrophage cell lines were stimulated with the TLR ligands, and the production of the proinflammatory cytokine IL-6 in the culture supernatants was determined by ELISA (Fig. 2A). The expression of HCV structural proteins or NS5B
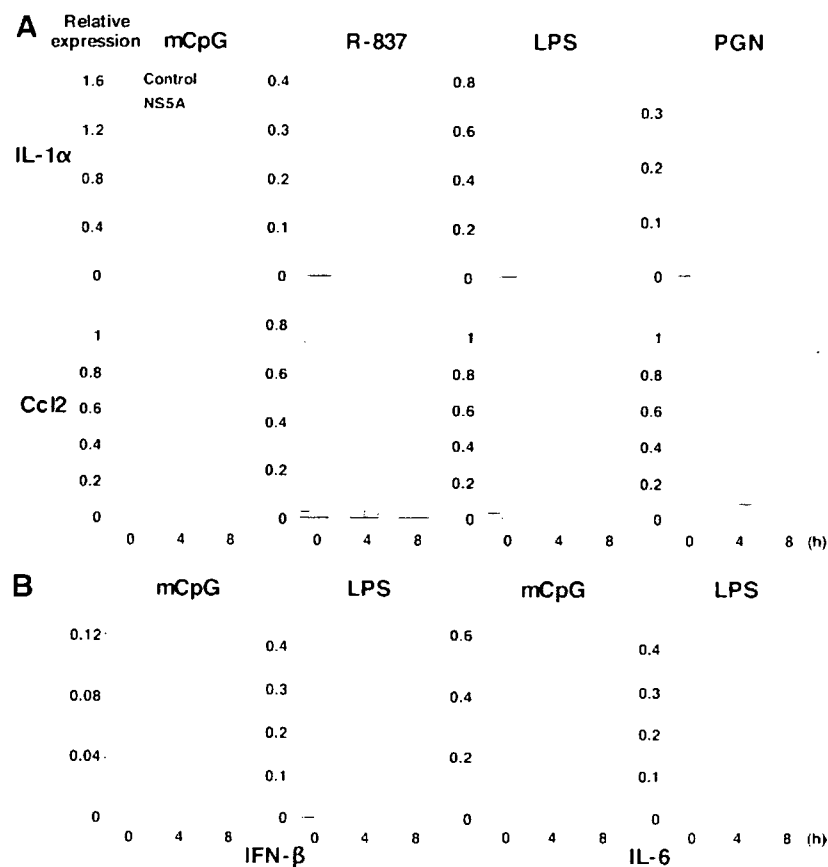
FIG. 3. Effect of NS5A expression on the production of cytokines and chemokines in response to TLR ligands in macrophage cell lines. Cells (3 × 10⁶ cells/well) were stimulated with 10 μg/ml of mCpG, 10 μg/ml of R-837, 25 ng/ml of LPS, and 10 μg/ml of PGN for the times indicated. Total RNA was extracted from macrophage cell lines expressing NS5A (gray bars) or control (white bars), and the expression of mRNA of IL-1α and Ccl2 (A) and IFN-β and IL-6 (B) was determined by real-time PCR.

had no effect on IL-6 production after stimulation with mCpG, R-837, LPS, or PGN, which are ligands for TLR9, TLR7, TLR4, and TLR2, respectively. On the other hand, the expression of NS3, NS3/4A, NS4B, or NS5A inhibited the production of IL-6 induced by treatment with the ligands. These results indicate that the expression of NS3, NS3/4A, NS4B, and NS5A inhibits the production of IL-6 through the TLR-dependent signaling pathway in macrophage cell lines.

In addition to proinflammatory cytokine production via NF-κB activation, stimulation of TLR also activates mitogen-activated protein kinases (MAPKs). We then examined the activation of ERK, a MAPK signaling pathway, in response to the TLR ligands in the macrophage cells expressing HCV proteins (Fig. 2B). Although the expression of the HCV structural proteins NS3, NS4B, and NS5B did not alter the phosphorylation status of ERK1/2 in response to stimulation with the TLR7 ligand R-837, the expression of NS5A exhibited a clear inhibition of the phosphorylation of ERK1/2. To further examine the effect of NS5A expression on the MAPK cascade in response to the TLR ligands, the cells were treated with mCpG, LPS, and PGN. NS5A expression was found to inhibit the phosphorylation of ERK1/2 in response to stimulation with the ligands for TLR9, TLR4, and TLR2 (Fig. 2C). In contrast, the phosphorylation of c-Jun NH₂-terminal kinase in

response to stimulation with R-837 was less impaired in the macrophage cell line expressing NS5A (data not shown). These results indicate that the expression of NS3, NS3/4A, NS4B, or NS5A inhibits the production of proinflammatory cytokines and that the expression of NS5A alone induces the inhibition of the MAPK cascade in response to stimulation by various TLR ligands in macrophage cells.

To further examine the effect of NS5A expression on the production of the other proinflammatory cytokines and chemokines in response to TLR ligands, the expression of mRNA of IL-1α and Ccl2 in cells expressing NS5A after stimulation with TLR ligands was determined by real-time PCR (Fig. 3A). Expression of IL-1α and Ccl2 was reduced in cells expressing NS5A by stimulation with mCpG, R-837, LPS, or PGN except for the IL-1α expression by treatment with LPS, probably due to the TRIF-dependent activation of NF-κB. To further confirm the specific inhibition of the MyD88-dependent signaling pathway by NS5A, we examined the effects of NS5A expression in macrophage cells on the MyD88-independent/TRIF-dependent production of IFN-β (Fig. 3B). Although the expression of IL-6 mRNA in cells expressing NS5A was impaired after stimulation with mCpG or LPS, the expression of IFN-β was enhanced. These results suggest that the expression of NS5A specifically inhibits the MyD88-dependent signaling pathway.

TLR-dependent and -independent immune activation of macrophage cells expressing NS3/4A or NS5A protein by RNA virus and dsRNA. TLR3 has been shown to sensitize cells in response to double-stranded RNA (dsRNA) generated by viral infection and a synthetic dsRNA analog, poly(I:C), through an adaptor molecule, TRIF/TICAM-1, but not MyD88. Furthermore, RIG-I and MDA5 have been identified as being cytoplasmic dsRNA detectors responding to poly(I:C) and viral RNAs (57, 58), sensitizing cells through an adaptor molecule, IPS-1/MAVS/VISA/CARDIF, in a TLR-independent manner (24, 35, 46, 55). Recently, HCV NS3/4A protease was shown not only to cleave HCV nonstructural proteins but also to inhibit viral RNA- and dsRNA-induced IFN production through the cleavage of the adaptor molecules TRIF (28) and IPS-1 (29, 30, 33, 35). Moreover, it has been shown that NS3/4A protease inhibits dsRNA-induced immune activation in a protease-dependent manner in human hepatoma cell lines (11).

To determine whether murine TRIF (mTRIF) is cleaved by HCV NS3/4A protease, C-terminally His-tagged mTRIF was coexpressed with N-terminally Flag-tagged NS3, NS3/4A, or NS3/4A(S139A) in 293T cells. Immunoblot analyses revealed that mTRIF was not processed by HCV NS3/4A protease, probably due to differences in the amino acid sequences at the cleavage site in mTRIF (Fig. 4A). Amino acid sequences at the cleavage site of human TRIF are Cys^{372} and Ser^{373}, and those at the cleavage sites of mTRIF are Pro^{372} and Ala^{373} (Fig. 4B). These results suggest that HCV NS3/4A protease could not inhibit immune activation through the TLR3-mTRIF-dependent signaling pathway in murine cells. We next determined the processing of IPS-1 by HCV NS3/4A protease. N-terminally Flag-tagged mIPS-1 or its C508A mutant, with Cys^{508} replaced with Ala to prevent cleavage by HCV NS3/4A protease, was coexpressed with N-terminally Flag-tagged NS3, NS3/4A, or NS3/4A(S139A) in 293T cells. Immunoblot analyses revealed that wild-type mIPS-1 was cleaved in cells coexpressing the active NS3/4A protease but not in those with NS3 (Fig. 4C). mIPS-1 processing was reduced in cells coexpressing NS3/4A(S139A) as well as in those coexpressing mIPS-1(C508A) and NS3/4A (Fig. 4C). Furthermore, we were able to detect cleavage of endogenous mIPS-1 in macrophage cell lines expressing NS3/4A but not in those expressing NS3 or NS3/4A(S139A) (Fig. 4D), indicating that mIPS-1 in murine macrophage cell lines is cleaved by HCV NS3/4A protease, as reported previously for a human hepatoma cell line.

We then examined the effect of expression of NS3/4A and NS5A on TLR-dependent and -independent immune activation induced by dsRNA. VSV and poly(I:C) were inoculated into macrophage cell lines, and the expression of mRNA of IFN-β and IL-1α was determined by real-time PCR (Fig. 4E). The macrophage cell lines expressing NS3/4A exhibited inhibition of IL-1α and IFN-β expression upon infection with VSV but not in response to poly(I:C), whereas no inhibition was observed in those expressing NS5A. These results suggest that the invasion of VSV and poly(I:C) is preferentially recognized in RAW cell lines by RIG-I–IPS-1- and TLR3-TRIF-dependent signaling pathways, respectively. Inhibition of IL-1α and IFN-β expression upon infection with VSV but not in response to poly(I:C) is probably due to the selective cleavage of IPS-1 but not TRIF by NS3/4A protease in the macrophage cell lines.

In contrast, the expression of NS5A has no effect on both TLR3-TRIF and RIG-I–IPS-1-dependent signaling pathways in macrophage cells.

Although MyD88/IRF7-dependent production of IFN-α upon activation was reported in plasmacytoid DCs (pDCs) (17, 23), it is unclear whether murine macrophage cells are capable of producing IFN-α in a TLR/MyD88/IRF7-dependent manner. To examine the effect of NS5A expression on IFN-α production, the expression of IFN-α1 and IFN-α4 in the macrophage cell line upon infection with VSV was determined (Fig. 4E, bottom). In contrast to the effect on IFN-β production, the expression of NS5A in the macrophage cells reduced the production of IFN-α1 and IFN-α4 upon infection with VSV, although the inhibitory effect was weaker than that of NS3/4A. These results suggest that RAW264.7 cells are capable of producing IFN-α in a TLR/MyD88/IRF7-dependent manner upon infection with VSV as reported for pDCs, and the expression of NS5A partially counteracts this signaling pathway. However, the production of type I IFNs by the treatment with ligands for TLR7 (R-837) and TLR9 (mouse CpG) was weaker than that induced by infection with VSV in macrophage cells (data not shown). Further study is needed to clarify the precise mechanisms of the inhibition of TLR/MyD88/IRF7-dependent IFN-α production by the expression of HCV NS5A in human immune cells.

NS5A interacts with MyD88 in mammalian cells. The inhibition of the production of proinflammatory cytokines and chemokines and the MAPK cascade by NS5A expression in response to stimulation by various TLR ligands without participation of TRIF- and IPS-1-dependent signaling pathways suggests that NS5A specifically inhibits the TLR-MyD88-dependent signaling pathway in macrophage cell lines. MyD88 is a critical component of the signaling pathway and leads to the production of proinflammatory cytokines, chemokines, and MAPKs. To determine the effect of the expression of HCV proteins on the TLR signaling pathway in macrophage cell lines, the interaction of the HCV proteins with the adaptor molecules in the signaling pathway of the TLR family was examined by immunoprecipitation analysis. His-tagged MyD88 was coexpressed with Flag-tagged HCV proteins in 293T cells and immunoprecipitated with the indicated antibodies. As shown in Fig. 5A and B, MyD88 was coimmunoprecipitated with NS5A but not with structural and other nonstructural proteins in 293T cells.

To further confirm the specificity of the interaction of NS5A with MyD88, NS5A was coexpressed with other adaptor molecules in the TLR signaling pathway, TRAM, TIRAP, or TRIF, in 293T cells (Fig. 5C). NS5A interacted with MyD88 but not other adaptor molecules, suggesting that NS5A may inhibit the production of proinflammatory cytokines and chemokines and the phosphorylation of MAPKs through the counteraction of the MyD88-dependent TLR signaling pathway.

NS5A interacts with the death domain of MyD88 through the ISDR and inhibits recruitment of IRAK to MyD88. To determine the region of NS5A responsible for the interaction with MyD88, a series of deletion mutants of N-terminal Flag-tagged NS5A was constructed, and its interaction with His-tagged MyD88 was examined (Fig. 6A). The NS5A mutant covering amino acids 1 to 280 but not that covering amino

A

mTRIF-myc-His　　+　+　+　+
Flag-NS3　　　　　+
Flag-NS3/4A　　　　　　+
Flag-S139A　　　　　　　　　+
　　　　kDa

IB: His　83 -　　　　　　　　　　　mTRIF

IB: Flag　　　　　　　　　　┌NS3/4A
　　　62 -　　　　　　　　　└─NS3

B

NS4A /4B	YREFDEMEEC	ASHLPYIEQ
NS4B/5A	WINEDCSTPC	SGSWLRDVW

　　　　　　　　372
Human TRIF　　PPPPPSSTPC　SAHLTPSSL
Mouse TRIF　　SSASSPSSYP　APPTSTSPV

　　　　　　　　508
Human IPS-1　RKFQEREVPC　HRPSPGALW
Mouse IPS-1　QQPQEEEEHC　ASSMPWAKW

C

Flag-mIPS-1　　+　+　+　+
Flag-C508A　　　　　　　+　+
Flag-NS3　　　　+
Flag-NS3/4A　　　　+　　　　+
Flag-S139A　　　　　　+
　　　　kDa

IB: mIPS-1　62 -　　　　　　━ ━ -mIPS-1
　　　　47.5 -　　　　　　━　-mIPS-1*

IB: NS3　　　　　　　　　　　　┌NS3/4A
　　　62 -　　　　　　　　　　└─NS3

D

　　　　kDa
IB: mIPS-1　62 -　　　　　　　　　　-mIPS-1
　　　47.5 -　　　　　　　　　　　　-mIPS-1*

IB: NS3　　　　　　　　　　　　　┌NS3/4A
　　62 -　　　　　　　　　　　　　└─NS3

IB: β-actin　47.5 -　　　　　　　　　β-actin

E

IFN-β　　　　IL-1α　　　　IFN-β　　　　IL-1α

Relative expression

Control
NS3/4A
NS5A

VSV　　　　　　　　　poly:I-C

IFN-α1　　　　IFN-α4

Relative expression

VSV

FIG. 4. TLR-dependent and -independent immune activation of macrophage cells expressing theNS3/4A or NS5A protein by RNA virus and dsRNA. (A) Myc-His-mTRIF was coexpressed with Flag-NS3, -NS3/4A, or -NS3/4A(S139A) in 293T cells and immunoblotted (IB) with antibodies against His and Flag. (B) Alignment of the flanking sequence of NS3 protease cleavage sites of NS4A/4B, NS4B/5A, TRIF, and IPS-1 of human and murine origins. The cleavage site is indicated by an arrow. (C) Flag-mIPS-1 and a mutant with Cys508 replaced with Ala (C508A) were coexpressed with Flag-NS3, -NS3/4A, or -NS3/4A(S139A) in 293T cells and immunoblotted with antibodies against mIPS-1 and NS3. (D) Processing of endogenous mIPS-1. Cell lysates of the macrophage cell lines expressing NS3, NS3/4A, and NS3/4A(S139A) were immunoblotted with antibodies against mIPS-1. NS3, and β-actin. The cleavage product of mIPS-1 is indicated as mIPS-1* . (E) Cells (3 × 10⁶ cells/well) were stimulated with 2 × 10⁵ PFU/ml of VSV or 50 μg/ml of poly(I:C) for the times indicated. Total RNA was extracted from the macrophage cell lines expressing NS3/4A (black bars), NS5A (gray bars). or control (white bars), and the expression of mRNA of IFN-β, IL-1α, IFN-α1. and IFN-α4 was determined by real-time PCR.
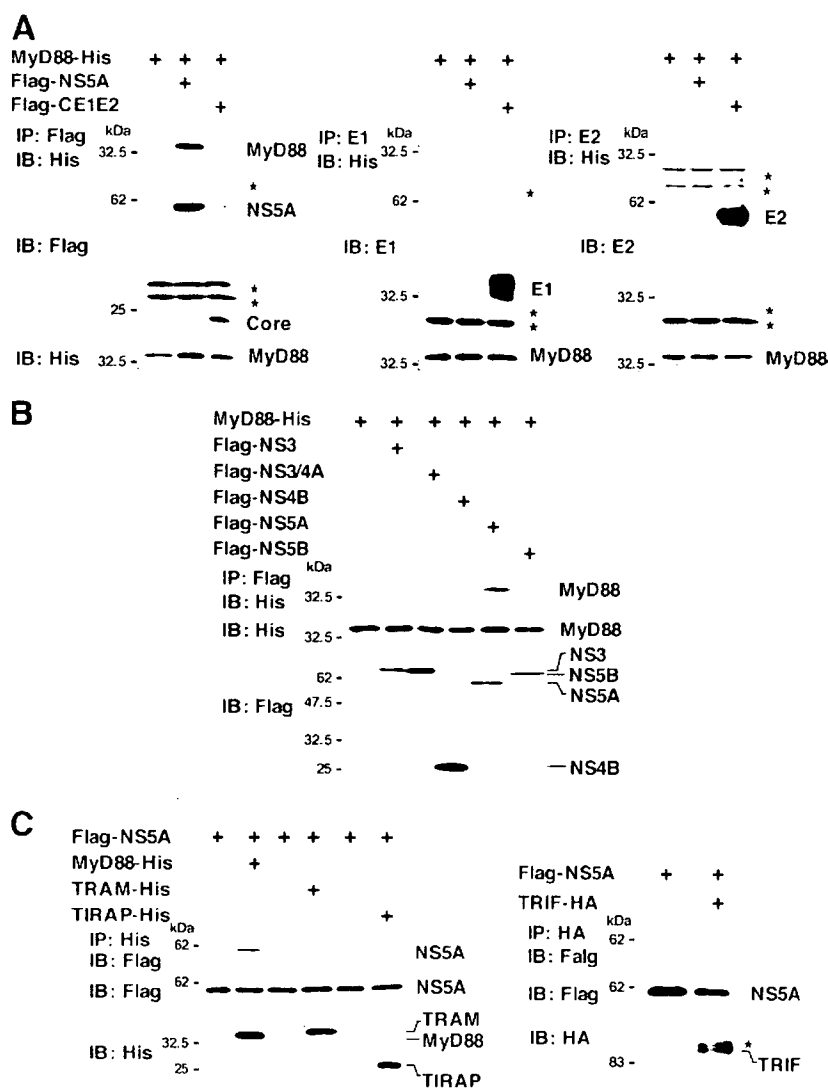
FIG. 5. NS5A interacts with MyD88. MyD88-His was coexpressed with Flag-core/E1/E2 or -NS5A (A) or Flag-NS3, -NS3/4A, -NS4B, -NS5A, or -NS5B (B) in 293T cells; immunoprecipitated (IP) with anti-Flag, E1, or E2 antibody; and immunoblotted (IB) with anti-His antibody. (C) Flag-NS5A was coexpressed with MyD88-His, TRAM-His, TIRAP-His, or TRIF-HA in 293T cells and immunoprecipitated with anti-His or -HA antibody. The immunoprecipitates were immunoblotted with anti-Flag antibody. Asterisks indicate nonspecific bands.

acids 1 to 200 exhibited binding to MyD88, suggesting that amino acid residues 200 to 280 of NS5A are required for the interaction with MyD88. Further mutational analyses of NS5A revealed that amino acid residues 240 to 280, which overlap the ISDR (amino acid residues 237 to 276), which was previously suggested to be involved in IFN resistance (10, 41), are required for the interaction with MyD88 (Fig. 6A). To determine the region of MyD88 responsible for the interaction with NS5A, His-tagged MyD88 mutants were coexpressed with Flag-tagged NS5A in 293T cells and immunoprecipitated with anti-His antibody. A MyD88 deletion mutant lacking amino acids 1 to 50, but not one lacking amino acids 1 to 80, and a mutant possessing amino acids 1 to 70 exhibited binding to NS5A, suggesting that amino acid residues 50 to 70 in the death domain of MyD88 are required for the interaction with NS5A (Fig. 6B).

MyD88 associates with TLRs and acts as an adapter that recruits IRAK, which is known as a key regulator for TLR7- and TLR9-mediated IFN-α production in pDCs (53). To determine the role of NS5A binding to MyD88 in the TLR-MyD88-dependent signaling pathway, we examined the association of IRAK with MyD88 in the presence of NS5A. Flag-tagged MyD88 was coexpressed with Myc-tagged IRAK-1 or IRAK-4 and immunoprecipitated with anti-Myc antibody (Fig. 6C, left). IRAK-1, but not IRAK-4, was coimmunoprecipitated with MyD88. Although NS5A did not bind to IRAK-1, it was not possible to assess the interaction of NS5A with IRAK-4 due to the degradation of NS5A in cells coexpressing IRAK-4 for unknown reasons (Fig. 6C, middle). To examine the interplay between IRAK-1 and MyD88 in the presence of NS5A. Flag-tagged MyD88 and Myc-tagged IRAK-1 were coexpressed with Flag-tagged NS5A in 293T cells. The interaction

A

Domain I   Domain II   Domain III

1(1973)   221   276   336   376   447(2419)

N-terminal amphipathic helix   Hyperphosphorylation cluster   ISDR (237-276 aa)   Polyproline cluster

MyD88 binding region   240-280 aa

MyD88-His   + + + + +
Flag-NS5A + +
Flag-1-353   +
Flag-1-280   +
Flag-1-200   +
Flag-1-100   +
kDa

IP: His   32.5 -   NS5A
IB: Flag

47.5 -
IB: Flag   32.5 -   NS5A

IB: His   32.5 -   MyD88

MyD88-His   + + + +
Flag-NS5A   +
Flag-Δ240-280   +
Flag-Δ280-300   +
kDa

IP: Flag
IB: His   32.5 -   MyD88

62 -
IB: Flag   47.5 -   NS5A

IB: His   32.5 -   MyD88

B

Flag-NS5A   + + + + + + +
MyD88-His   +
ΔN1-His   +
ΔN2-His   +
ΔN3-His   +
ΔC1-His   +
ΔC2-His   +
ΔC3-His   +
kDa
IP: His   62 -   NS5A
IB: Flag

32.5 -
IB: His   MyD88

IB: Flag   62 -   NS5A

Death Domain   Toll Domain

MyD88   32   110 161   296
ΔN1   50
ΔN2   80
ΔN3   130
ΔC1   150
ΔC2   100
ΔC3   70

50-70 aa   NS5A binding region

C

Flag-MyD88   + + +
IRAK-1-Myc   +
IRAK-4-Myc   +
kDa
IP: Myc
IB: Flag   32.5 -   MyD88

IB: Flag   32.5 -   MyD88

83 -   IRAK-1
IB: Myc   62 -
   IRAK-4
47.5 -

Flag-NS5A   + + +
IRAK-1-Myc   +
IRAK-4-Myc   +
kDa
62 -   NS5A

62 -   NS5A

83 -   IRAK-1
62 -

IRAK-4
47.5 -

Flag-NS5A   + + +
IRAK-1-Myc   + + + +
Flag-MyD88   + + + +
kDa
IP: Myc
IB: Flag   32.5 -   MyD88

IB: Flag   32.5 -   MyD88

IB: Flag   62 -   NS5A
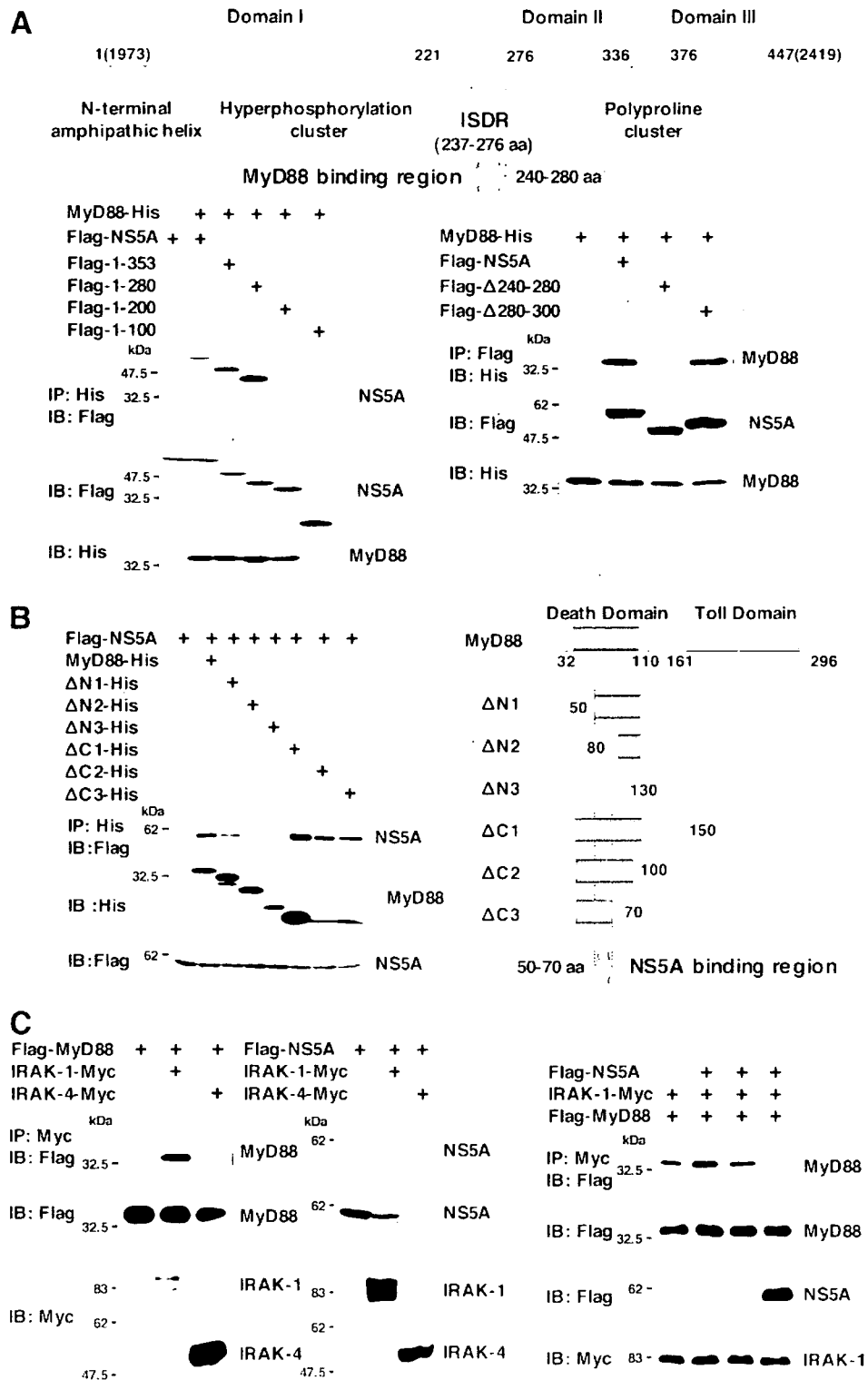
IB: Myc   83 -   IRAK-1

FIG. 6. NS5A interacts with the death domain of MyD88 through the ISDR and inhibits recruitment of IRAK to MyD88. (A) The structure of NS5A and the MyD88 binding region are indicated at the top. MyD88-His was coexpressed with C-terminal deletion mutants of Flag-NS5A in 293T cells, immunoprecipitated (IP) with anti-His antibody, and immunoblotted (IB) with anti-Flag antibody (left). MyD88-His was coexpressed with Flag-NS5A deletion mutants (Δ240-280 or Δ280-300) in 293T cells, immunoprecipitated with anti-Flag antibody, and then immunoblotted with anti-His antibody (right). (B) Flag-NS5A was coexpressed with N-terminal or C-terminal deletion mutants of MyD88-His (ΔN1, ΔN2, ΔN3, ΔC1, ΔC2, or ΔC3) in 293T cells, immunoprecipitated with anti-His antibody, and immunoblotted with anti-Flag antibody. The structures of MyD88 and the deletion mutants and the NS5A binding region are indicated on the left. (C) Flag-MyD88 (left) or Flag-NS5A (middle) was coexpressed with IRAK-1-Myc or IRAK-4-Myc in 293T cells, immunoprecipitated with anti-Myc antibody, and immunoblotted with anti-Flag antibody. Flag-MyD88 and IRAK-1-Myc were coexpressed with Flag-NS5A in 293T cells, immunoprecipitated with anti-Myc antibody, and immunoblotted with anti-Flag antibody. The effect of the increase in Flag-NS5A expression on the interaction of MyD88 with IRAK-1 was examined by transfection with 0.1, 0.5, or 2 μg of Flag-NS5A expression plasmid (right).

A

MyD88-His   +   +   +   +
Flag-NS5A(J1)   +
Flag-NS5A(H77c)   +
Flag-NS5A(JFH1)   +

IP: Flag   kDa
IB: His   32.5 -   MyD88

IB: His   32.5 -   MyD88

IB: Flag   62 -   ⌐NS5A(JFH1) / NS5A(H77c) \ NS5A(J1)

B

MyD88-His   +   +   +   +   +
Flag-NS5A(H77c)   +
Flag-Δ240-280(H77c)   +
Flag-NS5A(JFH1)   +
Flag-Δ240-280(JFH1)   +

IP: Flag   kDa
IB: His   32.5 -   MyD88

IB: His   32.5 -   MyD88

IB: Flag   62 -   ⌐NS5A(JFH1) / Δ240-280(JFH1) \ NS5A(H77c) ⌐Δ240-280(H77c)

C

237   ISDR   276

		230	240	250	260	270
H77c	(1a)	SASQLSAPSL	KATCTANHDS	PDAELIEANL	LWRQEMGGNI	TRVESENKVV
J1	(1b)	SASQLSALSL	KATCTTHHGA	PDTDLIEANL	LWRQEMGGNI	TRVESENKIV
Con1	(1b)	SASQLSAPSL	KATCTTRHDS	PDADLIEANL	LWRQEMGGNI	TRVESENKVV
JFH1	(2a)	SVSQLSAPSL	RATCTTHSNT	YDVDMVDANL	LMEGGVAQTE	PESRVPVLDF
		* ***** **	****	*	*** *	

D

   mCpG   R-837   LPS   PGN

■ Control
■ NS5A (J1)
▨ NS5A (H77c)
NS5A (JFH1)

IL-6 (ng/ml)

mCpG: 1.6, 1.2, 0.8, 0.4, 0
    5   1   0.2

R-837: 12, 10, 8, 6, 4, 2, 0
    20   4   0.8

LPS: 3, 2, 1, 0
    0.6   0.06   0.006
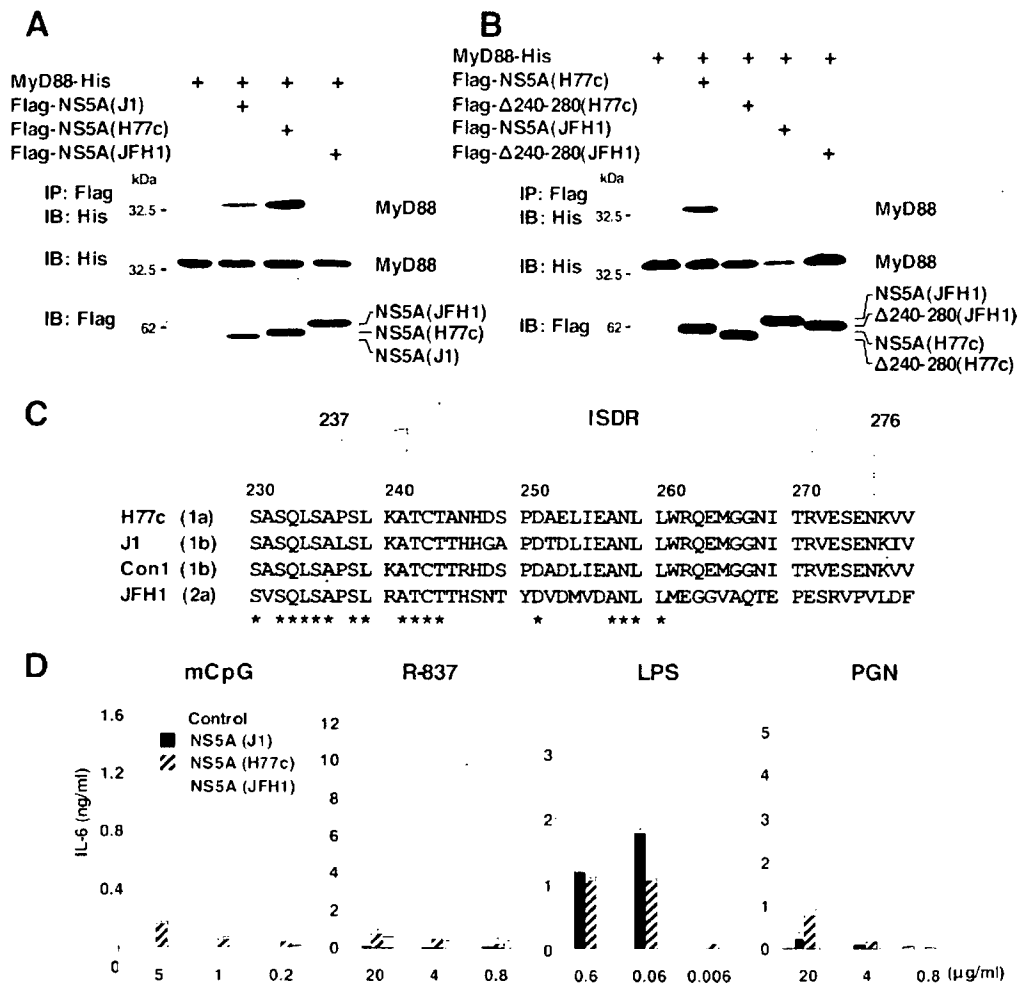
PGN: 5, 4, 3, 2, 1, 0
    20   4   0.8 (µg/ml)

FIG. 7. NS5A of other genotypes also interacts with MyD88 and inhibits the TLR signaling pathway. (A) Flag-NS5As of other genotypes were coexpressed with MyD88-His in 293T cells, immunoprecipitated (IP) with anti-Flag antibody, and immunoblotted (IB) with anti-His antibody. (B) The wild type or a deletion mutant lacking amino acids 240 to 280 of Flag-NS5A of genotype 1a or 2a was coexpressed with MyD88-His in 293T cells, immunoprecipitated with anti-Flag antibody, and immunoblotted with anti-His antibody. (C) Amino acid sequences of ISDR and its adjacent region of strains H77c (genotype 1a), J1 (genotype 1b), Con1 (genotype 1b), and JFH1 (genotype 2a). The conserved amino acids among genotypes 1a and 1b are indicated by boxes. Conserved amino acids among all strains are indicated by asterisks. (D) Macrophage cell lines expressing NS5A of genotypes 1a (H77c), 1b (J1), and 2a (JFH1) were established. Cells were stimulated with the indicated amounts of mCpG, R-837, LPS, or PGN, and the production of IL-6 in the culture supernatants was determined by ELISA 24 h after stimulation. Data are shown as the means ± SD.

of IRAK-1 and MyD88 decreased in accord with the increasing NS5A expression complex (Fig. 6C, right), suggesting that the expression of NS5A may interfere with the TLR-MyD88-dependent signaling pathway through the inhibition of the recruitment of IRAK-1 to MyD88.

NS5A of other genotypes also interacts with MyD88 and inhibits the TLR signaling pathway. To determine the interaction of MyD88 with NS5A of other genotypes, Flag-tagged NS5A of genotype 1a (H77c) or 2a (JFH1) was coexpressed with His-tagged MyD88 in 293T cells. MyD88 was coprecipitated with the NS5As of genotypes 1a and 2a, although it should be noted that the interaction between the MyD88 and NS5A of genotype 2a was weaker than that of the other genotypes (Fig. 7A). To determine the region of the NS5As of genotype 1a or 2a responsible for the interaction with MyD88, N-terminal Flag-tagged NS5As of genotype 1a or 2a deletion

mutants lacking amino acids 240 to 280 (Δ240-280) were constructed, and their interaction with MyD88 was examined. Mutational analyses revealed that amino acid residues 240 to 280 of the NS5As of genotypes 1a and 2a were also required for the interaction with MyD88 (Fig. 7B). Amino acid alignment of the ISDRs of genotypes 1a, 1b, and 2a revealed that the region of genotype 2a was less conserved than those of the other genotypes (Fig. 7C).

To determine the effect of NS5A expression of other genotypes on the TLR signaling pathway, we established macrophage cell lines expressing NS5A of each genotype. NS5A expression for all genotypes was found to inhibit IL-6 production after stimulation with mCpG, R-837, LPS, or PGN (Fig. 7D). Although the association of NS5A of genotype 2a to MyD88 was weaker than that of other genotypes, the expression of genotype 2a NS5A in macrophage cells exhibited com-